EUKARYOTIC CELL, Apr. 2006, p. 696–711 Vol. 5, No. 4
1535-9778/06/$08.00+0 doi:10.1128/EC.5.4.696–711.2006
Copyright © 2006, American Society for Microbiology. All Rights Reserved.

Flagellar Motility Contributes to Cytokinesis in *Trypanosoma brucei* and Is Modulated by an Evolutionarily Conserved Dynein Regulatory System†

Katherine S. Ralston,[1] Alana G. Lerner,[1] Dennis R. Diener,[2] and Kent L. Hill[1,3]*

Department of Microbiology, Immunology, and Molecular Genetics, University of California, Los Angeles, California 90095[1]; Department of Molecular, Cellular and Developmental Biology, Yale University, New Haven, Connecticut 06520[2]; and Molecular Biology Institute, University of California, Los Angeles, California 90095[3]

Received 14 January 2006/Accepted 18 January 2006

The flagellum of *Trypanosoma brucei* is a multifunctional organelle with critical roles in motility and other aspects of the trypanosome life cycle. Trypanin is a flagellar protein required for directional cell motility, but its molecular function is unknown. Recently, a trypanin homologue in *Chlamydomonas reinhardtii* was reported to be part of a dynein regulatory complex (DRC) that transmits regulatory signals from central pair microtubules and radial spokes to axonemal dynein. DRC genes were identified as extragenic suppressors of central pair and/or radial spoke mutations. We used RNA interference to ablate expression of radial spoke (RSP3) and central pair (PF16) components individually or in combination with trypanin. Both *rsp3* and *pf16* single knockdown mutants are immotile, with severely defective flagellar beat. In the case of *rsp3*, this loss of motility is correlated with the loss of radial spokes, while in the case of *pf16* the loss of motility correlates with an aberrant orientation of the central pair microtubules within the axoneme. Genetic interaction between trypanin and PF16 is demonstrated by the finding that loss of trypanin suppresses the *pf16* beat defect, indicating that the DRC represents an evolutionarily conserved strategy for dynein regulation. Surprisingly, we discovered that four independent mutants with an impaired flagellar beat all fail in the final stage of cytokinesis, indicating that flagellar motility is necessary for normal cell division in *T. brucei*. These findings present the first evidence that flagellar beating is important for cell division and open the opportunity to exploit enzymatic activities that drive flagellar beat as drug targets for the treatment of African sleeping sickness.

African trypanosomes are parasitic protozoa that are infectious to humans and a broad range of animals. *Trypanosoma brucei* is transmitted by the tsetse fly and is the causative agent of African trypanosomiasis in humans, also known as "African sleeping sickness." Since *T. brucei* is an extracellular pathogen, the parasite relies on its own cell motility throughout its life cycle in both insect and mammalian hosts (18). In the insect vector, the parasite makes an ordered series of migrations through specific compartments to complete the developmental changes necessary for survival in a mammalian host (66, 68). In mammalian hosts, *T. brucei* initially replicates in the bloodstream but eventually penetrates the blood vessel endothelium and invades the connective tissues and central nervous system, where it initiates events that are ultimately lethal (42, 45). If untreated, African sleeping sickness is 100% fatal, and the lethal course of the disease is directly linked to the presence of parasites in the central nervous system (42, 45). Thus, parasite migration to specific host tissues correlates directly with pathogenesis.

The driving force for cell motility in *T. brucei* is a single flagellum, which extends from the basal body, through the flagellar pocket and along the length of the cell body to which it is attached (17, 67). The *T. brucei* flagellar apparatus includes a canonical eukaryotic 9+2 axoneme and additional structures, such as the paraflagellar rod (PFR) and flagellum attachment zone (FAZ), which are unique to trypanosomes and a few closely related protozoa (9, 17). Within the eukaryotic axoneme, it is well established that ATP-dependent dynein motors drive the sliding of adjacent outer doublet microtubules, providing the force for flagellar movement (11, 57). To generate complex flagellar waveforms, the activity of these dynein motors must be precisely coordinated both temporally and spatially, since simultaneous activation of all dynein arms would lead to a rigor-like state (11, 57). Dynein activity must also be coordinated with environmental sensory perception, since changes in the flagellar beat form, such as wave reversal and hyperactivated motility, are often associated with physiological responses to environmental cues (32, 36, 64). The identification of proteins and mechanisms underlying dynein regulation is one of the major challenges in cell biology.

In *T. brucei*, beating of the flagellum initiates at the distal tip and is propagated toward the base, pulling the cell forward in an auger-like spiraling motion with the flagellar tip leading (see video S1 in the supplemental material) (18, 69, 70). This implies the need for specialized dynein regulatory inputs because in most other organisms the flagellar beat propagates from the base to the tip (22). In some trypanosomatids, the flagellar beat direction is reversible and is modulated in response to extracellular cues (23, 64). In addition to its role in cell motility, the trypanosome flagellum is required for attachment to epithelial cells in the tsetse fly salivary gland (68) and plays structural roles in organelle inheritance, the establishment of cell polarity, and cleavage furrow formation (28, 37, 38, 52, 53). Thus, the trypanosome flagellum is a complex and

* Corresponding author. Mailing address: Department of Microbiology, Immunology and Molecular Genetics, University of California, Los Angeles, 609 Charles E. Young Dr., Los Angeles, CA 90095. Phone: (310) 267-0546. Fax: (310) 206-5231. E-mail: kenthill@mednet.ucla.edu.

† Supplemental material for this article may be found at http://ec.asm.org/.

dynamic organelle with critical roles throughout the parasite life cycle. Unfortunately, our current understanding of the *T. brucei* flagellum is primarily restricted to a few major structural proteins, and very little is known about proteins that regulate flagellar beat. Given the importance of motility and the flagellar apparatus in *T. brucei* development and disease pathogenesis, this represents a critical gap in our understanding of these deadly pathogens.

One protein that may play a role in regulating flagellar motility in *T. brucei* is trypanin, a 54-kDa coiled-coil protein that is tightly associated with the flagellar cytoskeleton and is required for normal flagellar motility (19, 26). Trypanin knockdown mutants have actively beating flagella but are unable to coordinate flagellar beat to drive productive directional motion and are thus only able to spin and tumble in place (26). Trypanin homologues are found in most if not all organisms, ranging from *Giardia lamblia* to humans, that contain a motile flagellum but are absent in organisms that lack motile cilia or flagella, such as *Caenorhabditis elegans*, which contains only nonmotile sensory cilia (9a, 19; K. L. Hill, unpublished observation).

We previously reported that *Chlamydomonas reinhardtii* contains a trypanin homolog (19). Rupp and Porter recently identified the *C. reinhardtii* trypanin homolog, PF2, in a screen for mutants that affect a dynein regulatory complex (DRC) that transmits signals from central pair (CP) and radial spoke (RS) complexes to axonemal dynein (55). PF2 has been suggested to provide a scaffold for DRC assembly on the axoneme (55), and consistent with this, the human homologue binds microtubules directly (J. M. Bekker, J. R. Colantonio, A. D. Stephens, W. T. Clarke, S. J. King, K. L. Hill, and R. H. Crosbie, submitted for publication). DRC genes were originally identified through the isolation of extragenic suppressors that restore flagellar beat to CP/RS mutants without restoring the missing structures (24). Isolation of these suppressors revealed the presence of a regulatory system that controls dynein activity on at least two levels (24). One group of suppressor mutations (*sup$_{pf}$3*, *sup$_{pf}$4*, *sup$_{pf}$5*, *pf2*, and *pf3*) are required for assembly of the DRC, which is localized adjacent to inner arm dynein I1 at the base of the second radial spoke in the 96-nm repeating unit of the axoneme (16, 24, 34, 43, 44). A second group of suppressors correspond to mutations in outer and inner arm dynein heavy chains (46, 47, 54). The presence of this axonemal dynein regulatory system is further supported by a variety of biochemical and ultrastructural studies (41, 61, 72). Together, these data have led to a model in which the DRC acts as a reversible inhibitor of axonemal dynein that is regulated by signals delivered via the central pair and radial spokes (48). In many organisms, the CP rotates within the axoneme, and this is thought to provide a means for distributing regulatory signals to dyneins arranged around the outer doublets (40, 71, 72). In the absence of CP/RS, the DRC constitutively inhibits dynein, leading to flagellar paralysis or erratic twitching (24, 43). Loss of the DRC releases dynein inhibition, thus partially suppressing CP/RS beat defects, although suppressed mutants do not regain wild-type motility (24, 43, 44, 48). Partial suppression reflects the fact that the DRC represents only one level of dynein regulation provided by the CP/RS system (24).

To determine whether a DRC-like regulatory system operates as a conduit for transmission of regulatory signals between the CP/RS apparatus and axonemal dynein in *T. brucei*, we used RNA interference (RNAi) to knock down the expression of radial spoke (RSP3) and central pair (PF16) components individually or in combination with trypanin. Our results demonstrate that radial spoke and central pair components are required for motility in *T. brucei*. We also report that CP microtubules exhibit a fixed orientation relative to outer doublet microtubules in wild-type trypanosomes, whereas in *pf16* and *pf20* mutants the CP orientation is highly variable. Importantly, trypanin behaves as a DRC component since the loss of trypanin suppresses the flagellar beat defect of a central pair mutant. Therefore, the DRC is an evolutionarily conserved dynein regulatory system, and trypanin is a component of this system in *T. brucei*. Surprisingly, we also discovered that flagellar motility is required for cytokinesis in *T. brucei*, since motility mutants defective in three distinct flagellar substructures all have difficulty completing cytokinesis.

MATERIALS AND METHODS

Cell culture and transfection. Procyclic culture form (PCF) 29-13 cells, which stably express T7 RNA polymerase and tetracycline (Tet) repressor (74), were used to generate all RNAi knockdown mutants. Trypanosomes were cultivated and stably transfected as described previously (20, 26). Clonal cell lines were obtained by limiting dilution. Clonal lines harboring the RNAi constructs p2T7^{-Ti-B}/RSP3, p2T7^{-Ti-B}/PF16, p2T7^{-Ti-B}/PF20, p2T7^{-Ti-B}/PFR2-1, p2T7^{-Ti-B}/PFR2-2, p2T7^{-Ti-B}/TPN, p2T7^{-Ti-B}/RSP3-TPN, or p2T7^{-Ti-B}/PF16-TPN (see section on DNA constructs, below) are referred to as TbRSP3, TbPF16, TbPF20, TbPFR2-1, TbPFR2-2, TbTPN, TbRSP3/TPN, and TbPF16/TPN, respectively. For tetracycline induction, cells were split into two flasks and cultured with or without 1 μg of tetracycline/ml and diluted as necessary to maintain exponential growth. For growth curves, cell densities were measured by using a hemacytometer, and the averages of two independent counts are reported. For knockdown mutants, clusters of up to four distinguishable cell bodies were counted. To culture cells with physical shaking, TbRSP3 cells were split into flasks with or without tetracycline and placed on an orbital shaker set at 80 rpm.

Database searches and multiple sequence alignments. *C. reinhardtii* protein sequences for RSP3 (accession number P12759) (73), PF16 (accession number AAC49169.1) (59), and PF20 (accession number AAB41727.1) (60) were used to identify homologues in the *T. brucei* genome database (http://www.sanger.ac.uk/cgi-bin/BLAST/submitblast/t_brucei/omni) by using WU-BLAST (Washington University, St. Louis, MI). Sequencing of the *T. brucei* genome was accomplished as part of the Trypanosoma Genome Network with support by The Wellcome Trust. We identified single-copy genes for RSP3 (GeneDB ID Tb11.47.0034), PF16 (GeneDB ID Tb927.1.2670), and PF20 (GeneDB ID Tb10.61.2920). The percent similarity of each *T. brucei* protein to its *C. reinhardtii* homologue is as follows: RSP3 (41.5% identity and 52.5% similarity), PF16 (55.9% identity and 69.2% similarity), and PF20 (37.3% identity and 50.6% similarity).

Multiple sequence alignments were performed with the CLUSTAL W algorithm (65) by using Vector NTI software (Vector NTI Advance Suite 8; InforMax, Inc., Bethesda, MD). For RSP3, the following proteins were aligned: *Homo sapiens* (accession number AAK26432), *C. reinhardtii* (accession number P12759), *T. brucei* (GeneDB ID Tb11.47.0034), *T. cruzi* (GeneDB ID Tc00.1047053506721.20), and *Leishmania major* (GeneDB ID LmjF27.0520). For PF16, the following proteins were aligned: *H. sapiens* (accession number CAH72210), *C. reinhardtii* (accession number AAC49169.1), *T. brucei* (GeneDB ID Tb927.1.2670), *T. cruzi* (GeneDB ID Tc00.1047053510955.40), and *L. major* (GeneDB ID LmjF20.1400). For PF20, the following proteins were aligned: *H. sapiens* (accession number AAM63956), *C. reinhardtii* (accession number AAB41727.1), *T. brucei* (GeneDB ID Tb10.61.2920), *T. cruzi* (GeneDB Tc00.1047053511277.340), and *L. major* (GeneDB ID LmjF18.0470).

DNA constructs. All RNAi plasmids were constructed in p2T7^{-Ti-B}, which contains opposing, tetracycline-inducible T7 promoters such that tetracycline-induced transcription generates an intermolecular double-stranded RNA (dsRNA) (30). To create p2T7^{-Ti-B}/RSP3, a 375-bp fragment corresponding to nucleotides (nt) 566 to 940 of the *T. brucei* RSP3 open reading frame (ORF) was PCR amplified from 29-13 genomic DNA and cloned in the forward orientation into the HindIII and SacII sites in p2T7^{-Ti-B}. To create p2T7^{-Ti-B}/PF16, a 247-bp fragment corresponding to nt 1288 to 1534 of the *T. brucei* PF16 ORF was PCR amplified from 29-13 genomic DNA and cloned in the forward orientation into

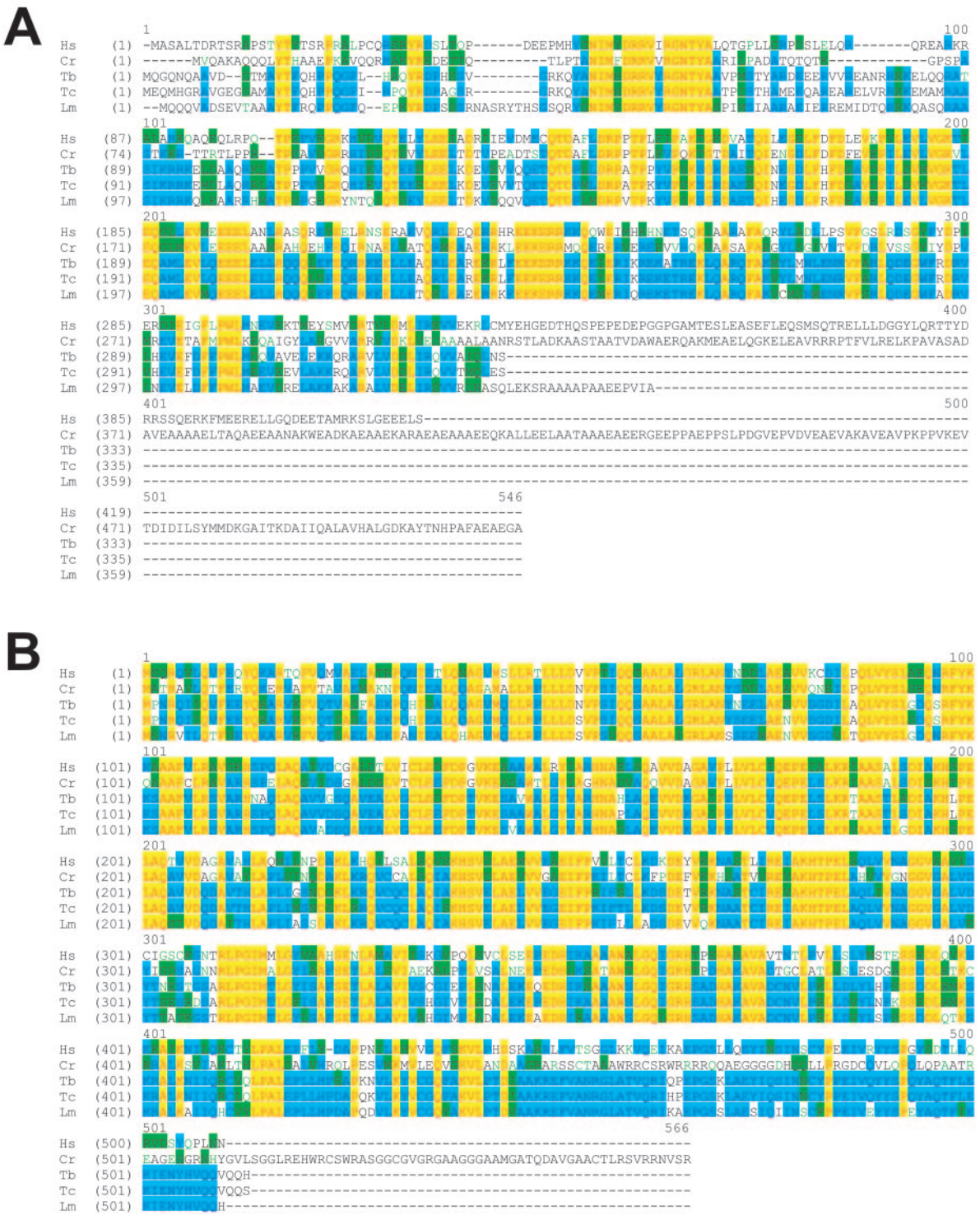

FIG. 1. RSP3, PF16, and PF20 protein alignments. Alignments of full-length RSP3 (A), PF16 (B), and PF20 (C) proteins from *Homo sapiens* (Hs), *C. reinhardtii* (Cr), *T. brucei* (Tb), *T. cruzi* (Tc), and *L. major* (Lm) are shown. Residues that are conserved in all four proteins are shaded yellow, while residues that are conserved in three or more proteins are shaded blue, and conservative substitutions are shaded green.

the SacII and XbaI sites in p2T7^{-Ti-B}. To create p2T7^{-Ti-B}/PF20, a 407-bp fragment corresponding to nt 291 to 697 of the *T. brucei* PF20 ORF was PCR amplified from 29-13 genomic DNA and cloned in the forward orientation into the SacII and XbaI sites in p2T7^{-Ti-B}. To create p2T7^{-Ti-B}/PFR2-1, a 448-bp fragment corresponding to nt 642 to 1089 of the *T. brucei* PFR2 ORF (GeneDB ID Tb08.5H5920) was PCR amplified from 29-13 genomic DNA and cloned in the forward orientation into the HindIII and BamHI sites in p2T7^{-Ti-B}. Note that this fragment of PFR2 was selected by RNAit (49) and is not expected to target PFR1 (GeneDB ID Tb03.26J7510) mRNA, since it does not contain any regions of identity to PFR1 longer than 12 nt. To create p2T7^{-Ti-B}/PFR2-2, a 1,723-bp

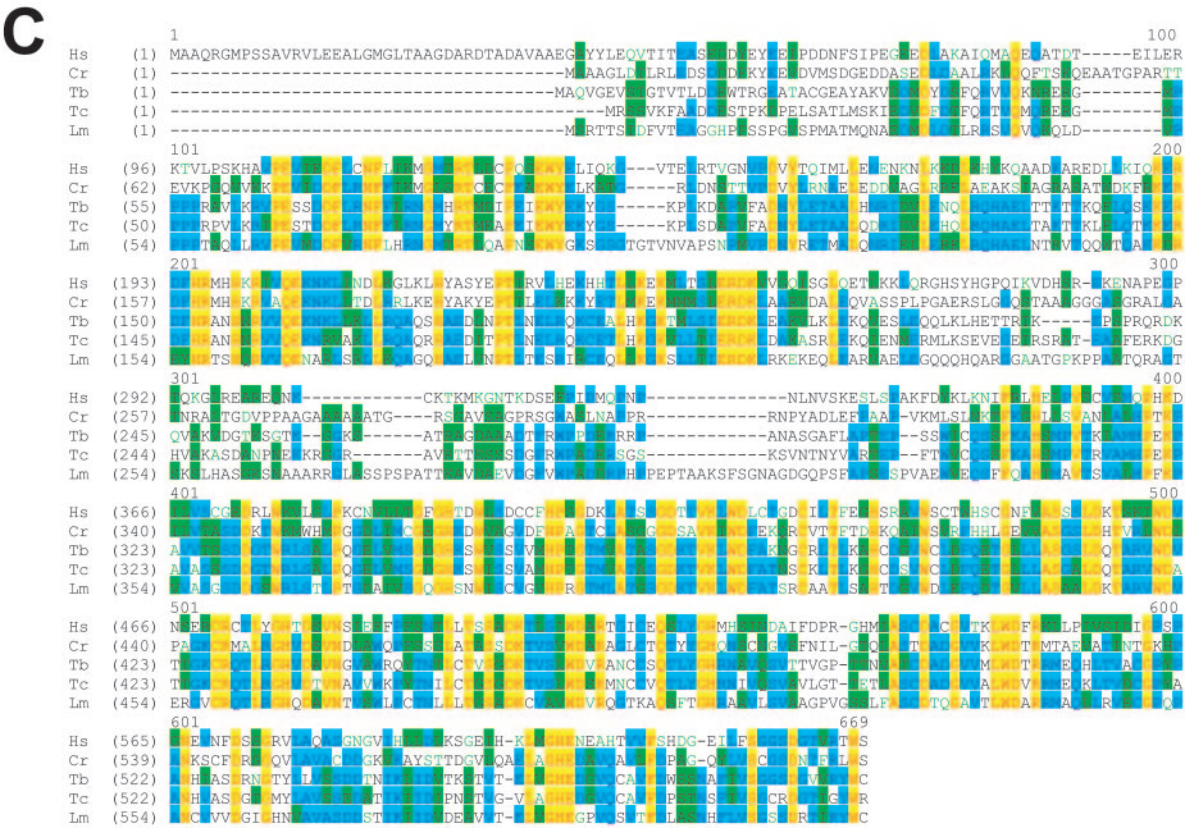

FIG. 1—*Continued.*

fragment corresponding to nt 78 to 1800 of the *T. brucei* PFR2 ORF was PCR amplified from 29-13 genomic DNA and cloned in the forward orientation into the HindIII and BamHI sites in p2T7^{-Ti-B}. This fragment of PFR2 is identical to the fragment used to create the *snl-2* cell line (4) and is similar to the fragments used to create *snl-1* (nt 78 to 1758) (7) and PFRAi (nt 78 to 1779) (14). To create p2T7^{-Ti-B}/TPN, a 252-bp fragment corresponding to nt 1103 to 1354 of the *T. brucei* trypanin ORF (26) was PCR amplified from 29-13 genomic DNA and cloned in the forward orientation into the BamHI and HindIII sites in p2T7^{-Ti-B}. All RNAi constructs were verified by restriction digestion and direct sequencing. Plasmids were linearized at the unique EcoRV or NotI site for transfection.

To create dual RNAi knockdown plasmids, tandem fragments of the targeted genes were cloned into p2T7^{-Ti-B}. To construct p2T7^{-Ti-B}/RSP3-TPN, the precise 375-bp RSP3 fragment that was used to create p2T7^{-Ti-B}/RSP3 was cloned in the forward orientation into the XbaI and BamHI sites, upstream of the TPN fragment in p2T7^{-Ti-B}/TPN. To create p2T7^{-Ti-B}/PF16-TPN, the precise 247-bp PF16 fragment that was used to create p2T7^{-Ti-B}/PF16 was cloned in the forward orientation into the XbaI and BamHI sites, upstream of the TPN fragment in p2T7^{-Ti-B}/TPN.

RNA preparation and Northern blotting. Total RNA samples were prepared by using an RNeasy kit (QIAGEN) according to the manufacturer's instructions. RNA samples (5 μg) were analyzed by Northern blotting as described previously (21). ^{32}P-labeled probes corresponding to nt 198 to 546 of the RSP3 ORF (RSP3 probe), nt 1288 to 1534 of the PF16 ORF (PF16 probe), nt 291 to 697 of the PF20 ORF (PF20 probe), nt 642 to 1089 of the PFR2 ORF (PFR2 probe), nt 1 to 775 of the TPN ORF (TPN probe), or the entire TRP ORF (TRP probe) were used. The TRP gene (GeneDB ID Tb09.244.2800) encodes a "trypanin-related protein" with 28% identity and 43% similarity to trypanin and will be described elsewhere (K. L. Hill, unpublished observation).

Sedimentation assays. Sedimentation assays were performed as described previously (6). Briefly, cells were incubated with or without tetracycline for 24 h and then resuspended to 5×10^6 cells/ml in fresh medium. Each culture was divided into aliquots to four cuvettes (1 ml per cuvette) and incubated under standard growth conditions. The optical density at 600 nm (OD_{600}) was measured every 2 h. At each time point, two cuvettes from each culture were left undisturbed to monitor sedimentation, while the other two cuvettes were resuspended to monitor growth. The ΔOD_{600} for each sample was calculated by subtracting the OD_{600} of the resuspended samples from that of the undisturbed samples.

Protein preparation and Western blotting. Protein extracts were prepared and analyzed by Western blotting (20). Trypanin was detected with a monoclonal antibody directed against a synthetic peptide corresponding to the last 13 amino acids of trypanin and was generated by an outside vendor (Cell Essentials, Cambridge, MA). PFR2 was detected with the monoclonal antibody L8C4 (29). The monoclonal antibody E7, directed against β-tubulin, was used as a control for protein loading. This antibody was developed (10) and obtained from the Developmental Studies Hybridoma Bank maintained by the University of Iowa Department of Biological Sciences.

Cell imaging. Live cells were imaged by using a Zeiss Axiovert 200 M inverted microscope with a 63× Achroplan LD or 63× Plan-Neofluor oil-immersion objective. Video images were captured as described below. For fluorescence microscopy, cells were imaged on a Zeiss Axioskop II compound microscope with a 63× Plan-Neofluor oil immersion objective, and images were captured by using a Zeiss Axiocam digital camera and Zeiss Axiovision 3.0 software.

Electron microscopy. TbRSP3, TbPF16, and TbPF20 cells were grown in the presence or absence of 1 μg of tetracycline/ml (96 h for TbRSP3 or 60 h for TbPF16 and TbPF20). Cytoskeletons or whole cells were prepared (19, 51) and then fixed for 60 min as described previously (26) with the addition of 1% (wt/vol) tannic acid. Samples were then washed in fixative without tannic acid and shipped overnight to Yale University, where processing was completed as described previously (58), except that staining en bloc was done in 2% uranyl acetate for 2 h.

Cytoskeletons were used for radial spoke analysis. Since a full complement of nine radial spokes was not always visible in all control sections, we established a blind assay to compare tetracycline-induced *rsp3* mutants to uninduced controls. Random silver sections from control (−Tet, $n = 32$) and tetracycline-induced (+Tet, $n = 31$) samples were scanned for axonemes in which the central pair microtubules were cut in cross section. These axonemes were photographed, and the images were coded and then mixed and scored blindly to determine the

number of spokes present per axoneme. After scoring, samples were decoded, and divided into control and tetracycline-induced groups, and the data are reported as the number of sections in each group having zero to nine spokes per section.

Whole-cell samples were used to measure the orientation of central pair microtubules in control cells and *pf16* and *pf20* mutants. Samples were selected randomly in which at least four outer doublet microtubules were clearly resolved. To measure central pair orientation, a reference line was drawn from the center point of outer doublet one to the center point of the outer doublet seven. The outer doublet seven can be readily identified by its attachment to the PFR (5). A line was then drawn that bisects the C1 and C2 central pair microtubules, and the angle of intersection of this line with the reference line was measured, moving clockwise from the reference line. The median angle in 45 control cells was 72°. For reference, this angle (72°) was set to zero, and the data were plotted as degrees deflection from zero.

Cell viability assay. TbRSP3 cells were incubated with or without tetracycline for 26 h and then subjected to a dye exclusion assay for cell viability (Molecular Probes Live/Dead Assay #L-3224) according to the manufacturer's instructions. Briefly, cells were washed once and resuspended to 2×10^7 cells/ml in 1× phosphate-buffered saline, and a 50-μl portion of the cells was then added to uncoated glass coverslips and incubated in 5 μM ethidium homodimer-1 in 1× phosphate-buffered saline for 30 min. Coverslips were inverted onto glass slides, sealed with nail polish, and imaged.

Immunofluorescence assays. To monitor cell cycle progression, cytoskeletons were prepared by detergent extraction (51) and subjected to immunofluorescence as described previously (26) with the α-PFR2 monoclonal antibody L8C4 (29). Anti-mouse secondary antibodies conjugated to Alexa-Fluor 488 (Molecular Probes) were used at a 1:400 dilution. Samples were mounted in Vectashield H-1200 (Vector Labs) containing 1.5 μg of DAPI (4′,6′-diamidino-2-phenylindole)/ml to visualize kinetoplast and nuclear DNA and then imaged. Cell cycle analysis was performed as described previously (58). Cells were distinguished as having one or two flagella (1F/2F), one or two kinetoplasts (1K/2K), and one nucleus or two discrete nuclei (1N/2N). A separate category (1mN) was used to distinguish cells with mitotic nuclei that contained a visible spindle. To minimize the influence of downstream defects, cells were examined 30 to 48 h postinduction, which corresponded to the onset of the cytokinesis defect.

Quantitation of cytokinesis in live cells. Live TbRSP3 cells, grown in the presence (+Tet, $n = 792$) or absence (−Tet, $n = 676$) of 1 μg of tetracycline/ml for 48 h were analyzed at the same cell densities in logarithmic growth, and two separate samples were quantified for each culture (+Tet, $n = 393$ and $n = 399$; −Tet, $n = 334$ and $n = 342$), with the standard deviation indicated by error bars. Note that the number of cells in cytokinesis was much higher in live cultures than in cells processed for immunofluorescence or harvested for routine cell counting. This indicated that cells undergoing cytokinesis were easily separated by physical manipulation. To account for this, live cultures were directly examined in culture flasks with minimal physical manipulation. Cells were categorized as having a single cell body or multiple physically attached cell bodies. Cells in which two cell bodies remain attached to one another ("double" in Fig. 4B) were further subdivided into three categories. "Double-1" corresponded to cells that had two full-length flagella but had not visibly begun cytokinesis (stages VI to VIII, as defined in Fig. 31 of reference 58). "Double-2" corresponded to cells that were in the middle-to-late stages of cytokinesis (stage IX in reference 58), while "double-3" corresponded to cells in the final stage of cytokinesis that were attached only by their extreme posterior ends (stage X in reference 58). Note that cells in each of these stages were also present in wild-type cultures (Fig. 4B) (58) and are therefore normal events in the *T. brucei* cell division cycle. The data shown are representative of three independent experiments.

Video microscopy of live cells. Videos are accessible in the supplemental material. *pf16* single and *pf16*/*tpn* double mutants (TbPF16 and TbPF16/TPN cells, respectively) were examined 48 h postinduction by using differential interference contrast (DIC) optics. Cells were visualized on standard glass slides, with double-sided tape between the slides and coverslips creating a chambered space to allow freedom of movement. Slides were inverted and examined through the coverslip. Videos were imaged by using a COHU charge-coupled device analog video camera and converted to digital format with a HandyCam (Sony, Inc.). Digital clips were captured at 30 frames per s and converted to AVI movies with Adobe Premiere Elements software (Adobe Systems). Representative examples are shown in in the supplemental material to illustrate the major phenotypes of each mutant. In Fig. 4A, images shown are single frames from videos S6 to S7 in the supplemental material. In Fig. 5C, the images shown are single frames from videos S9 and S10 in the supplemental material. Figure 8A and B are frames from videos S3 and S11 in the supplemental material, respectively. The frames were rotated to orient posterior end of the cell body upward.

Flagellar beat analysis. DIC video of live *pf16* single and *pf16*/*tpn* double mutants (TbPF16 and TbPF16/TPN cells, respectively) was captured 48 h postinduction as described above. For each cell line, footage of 100 random cells was recorded and analyzed. Since the flagellar beat in *T. brucei* is three-dimensional and bending can occur independently in the distal and proximal portions of the flagellum, it is difficult to reliably measure the frequency and amplitude of a single waveform along the length of the entire flagellum. Therefore, we measured the number of beats in each mutant over a 10-s period, focusing on the flagellar tip, where single mutants are most active. Beats of the flagellar tip were quantified over a 10-s time period for each cell. Where cells exhibited more than 12 beats in 10 s, individual flagellar movements could not be quantified, and these cells were categorized as ">12" beats/10 s, which is essentially continuous movement. An example of a *pf16* mutant that had >12 movements in this assay is shown in video S4 in the supplemental material to illustrate the qualitative differences between *pf16* and *pf16*/*tpn* mutants in the >12 category (see Fig. 8C).

RESULTS

RSP3, PF16, and PF20 are required for flagellar motility. We used RNAi to target radial spokes and the central pair apparatus of *T. brucei*. To target radial spokes, we chose RSP3, which is required for attachment of the spoke to the axoneme in *C. reinhardtii* (12). The major components of the central pair apparatus are two singlet microtubules, C1 and C2, together with their specific projections and intermicrotubule bridges (62). To target the central pair apparatus, we chose PF16 and PF20, which are localized to the C1 and C2 microtubule structures, respectively (59, 60) and are required for stability of central pair microtubules in *C. reinhardtii* (1, 15) and mice (56, 76).

BLAST searches of the *T. brucei* genome database identified single-copy RSP3, PF16 and PF20 homologues (see Materials and Methods). Protein alignments demonstrated that these proteins are highly conserved, with PF20 exhibiting the most divergence (Fig. 1). In the region of overlap, the percent identity among RSP3, PF16, and PF20 homologues are 27.9, 42.4, and 16.7%, respectively. The *C. reinhardtii* and human RSP3 proteins have unique C-terminal extensions of 201 and 90 amino acids, respectively, whereas the *C. reinhardtii* PF16 protein has a unique C-terminal extension of 52 amino acids, suggesting some aspects of their function may be organism specific. Notably, a shorter C terminus is also observed in RSP3 and PF16 from other kinetoplastids (Fig. 1A and B), and deletion studies in *C. reinhardtii* indicate that the C-terminal 140 amino acids of RSP3 are not required for motility (13).

Separate plasmids for tetracycline-inducible RNAi knockdown of RSP3, PF16, and PF20 were constructed, and stably transfected clonal cell lines were obtained by limiting dilution. These cell lines will be henceforth referred to as TbRSP3, TbPF16, and TbPF20 cells or interchangeably as *rsp3*, *pf16*, and *pf20* knockdown mutants. Northern blot analysis demonstrates that the targeted transcripts are dramatically reduced within 24 h of tetracycline induction (Fig. 2A). Likewise, visual inspection of *rsp3*, *pf16*, and *pf20* knockdown mutants revealed a severe motility defect within 24 h of induction (see below). To quantitate this defect, we performed sedimentation assays (Fig. 2B). All three mutants sedimented at a linear rate of approximately -0.03 OD_{600} units/hour, whereas uninduced cells remained suspended. A dye-based viability assay demonstrated that there was no difference in viability at the time of the assay (see Materials and Methods).

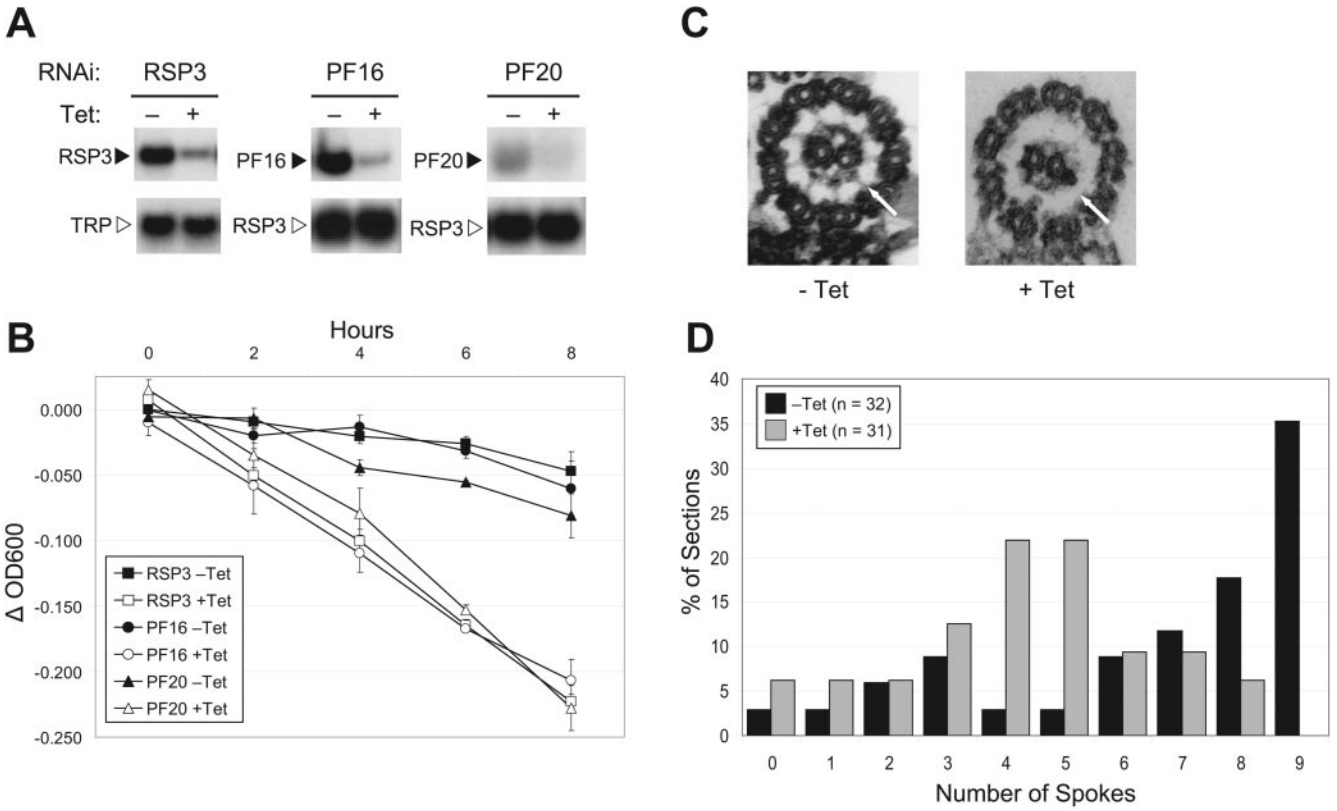

FIG. 2. RSP3, PF16, and PF20 are required for flagellar motility. (A) Northern blot demonstrating efficient RNAi knockdown of each target. TbRSP3, TbPF16, and TbPF20 cells were incubated in the presence (+) or absence (−) of tetracycline (Tet). Total RNA was prepared 24 h after the addition of tetracycline and subjected to Northern blot analysis with RSP3, PF16, or PF20 probes as indicated. The lower blots show loading controls. (B) Sedimentation assay demonstrating that *rsp3*, *pf16*, and *pf20* mutants have abnormal motility. TbRSP3, TbPF16, and TbPF20 cells were incubated in the presence (open symbols) or absence (filled symbols) of tetracycline for 24 h and assayed for sedimentation as described in Materials and Methods. The sedimentation curves represent the averages of two independent experiments, and error bars indicate the standard deviations. (C) Representative transmission electron micrographs of axonemes from TbRSP3 cells incubated with (+Tet) or without (−Tet) tetracycline. Arrows point out an example of a spoke in the −Tet sample and the equivalent position in the +Tet sample, where the spoke is absent. (D) Radial spokes are reduced but not completely absent in *rsp3* mutant axonemes. The number of spokes in electron microscopic sections of TbRSP3 cells incubated with or without tetracycline was determined. The percentages of sections with zero to nine spokes are shown.

Close examination revealed that *rsp3*, *pf16*, and *pf20* knockdown mutants were immotile in the sense that they exhibited no net movement in any direction, nor did they rotate or tumble as observed for trypanin knockdown mutants (26). However, a rudimentary flagellar beat or twitching was observed in all three mutants, so these cells should be considered "immotile" but not "paralyzed." This was particularly evident in *rsp3* mutants, where a few cells were completely paralyzed but most were able to sustain a rudimentary flagellar beat (video S2 in the supplemental material). Nonetheless, flagellar movement was generally confined to the distal portion of the flagellum, was mostly planar, and did not drive rotation of the cell body. Electron microscopy demonstrated that the number of spokes was reduced in axonemes of *rsp3* mutants compared to controls (Fig. 2C and D). In control cells, six or more spokes were clearly visible in 74% of sections ($n = 32$) compared to only 25% of sections from *rsp3* mutants ($n = 31$). The average number of spokes per section was reduced to 4.2 in *rsp3* mutants compared to 6.6 in controls.

pf16 and *pf20* mutants were also immotile and incapable of cellular rotation (videos S3 and S5 in the supplemental material). However, the beat defect was more severe than in *rsp3* mutants (compare videos S3 and S5 with video S2 in the supplemental material). Whereas *rsp3* mutants were able to sustain a modest flagellar beat, the *pf16* and *pf20* mutants only twitched erratically, and this irregular twitching was confined to the distal region of the flagellum. An additional feature shared by *pf16* and *pf20* mutants, but not *rsp3* mutants, was an exaggerated curvature in the cell body such that the flagellum tip and the anterior end of the cell were bent in an "S" shape toward the side of the cell opposite the flagellum (videos S3 and S5 in the supplemental material and Fig. 8A). In these cells, the flagellum was situated along the outer edge of the bend, such that flagellar movement decreased the degree of bending but was not powerful enough to fully straighten the cell body.

Electron microscopy of *pf16* and *pf20* mutants (Fig. 3) demonstrated a striking alteration in the orientation of the central pair microtubules. In control cells, central pair orientation within the axoneme was found to be restricted to a very narrow range, such that a plane bisecting the C1 and C2 microtubules was always roughly parallel to the paraflagellar rod viewed in

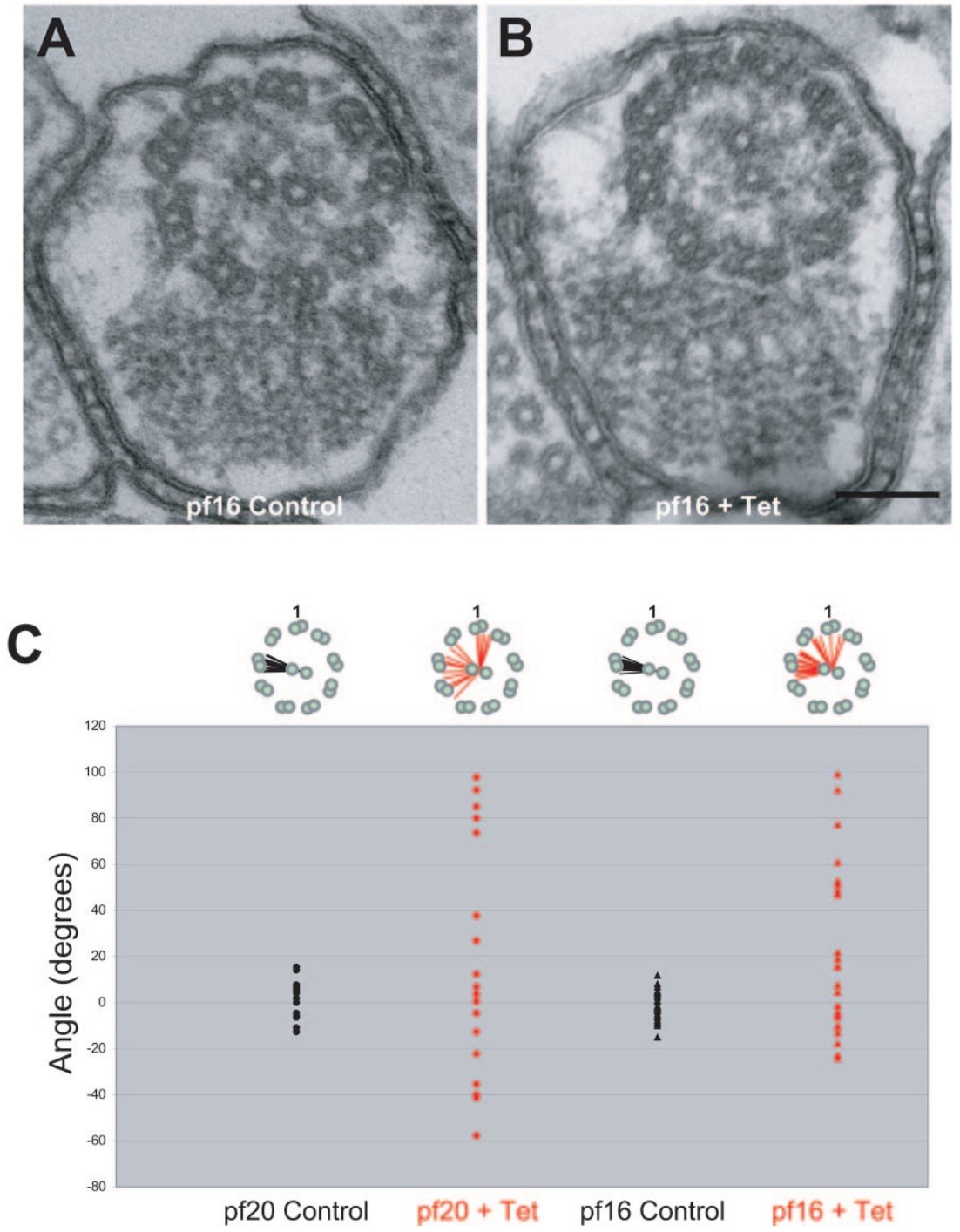

FIG. 3. The orientation of the central pair is variable in *pf16* and *pf20* mutants. (A and B) Representative electron microscopic images of flagella from TbPF16 cells grown in the absence (A, control) or presence (B, +Tet) of tetracycline. In the control cells (panel A), the central pair microtubules lie in a plane that is roughly parallel to the PFR, whereas in the *pf16* knockdown mutants (panel B) the central pair orientation is variable. Bar, 100 nm. (C) The central pair orientation was measured (see Materials and Methods) in *pf20* control cells ($n = 19$), pf20 mutants (+Tet, $n = 18$), *pf16* control cells ($n = 26$), and *pf16* mutants (+Tet, $n = 26$). For illustration purposes, the line bisecting C1 and C2 in each sample is depicted within a schematic diagram of the 9+2 axoneme at the top of the chart.

cross-section (Fig. 3A and C). In contrast, orientation of the central pair was highly variable in *pf16* and *pf20* mutants (Fig. 3B and C). Since we cannot distinguish between the two central pair microtubules, we do not know whether this represents random orientation through 360° or only 180°.

Flagellar motility is required for cytokinesis. RNAi knockdown of RSP3, PF16, and PF20 resulted in a severe motility defect that was evident within 24 h of tetracycline induction. Surprisingly, in all three mutants the loss of motility was invariably followed by a cell division defect such that cells failed

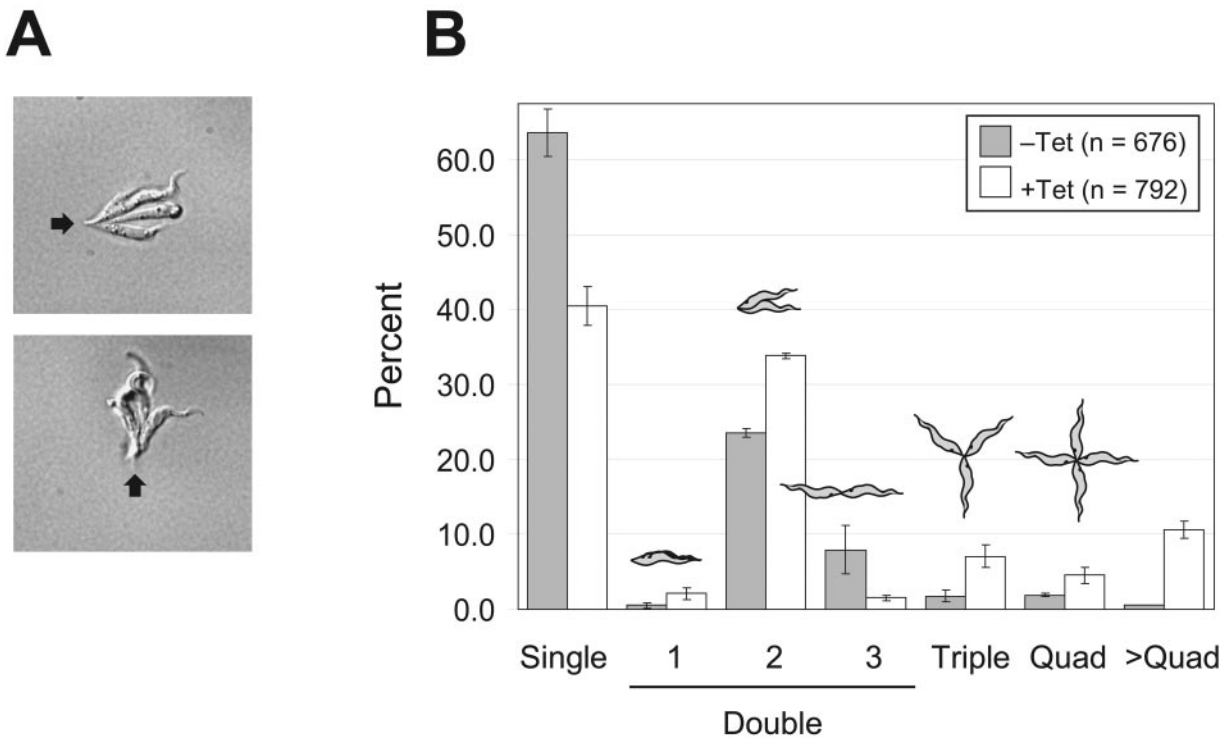

FIG. 4. *rsp3* mutants are defective in cytokinesis. (A) DIC images of live *rsp3* mutants in multicellular clusters 48 h after the addition of tetracycline (each image is a frame taken from videos S6 and S7 in the supplemental material). Small clusters of a few cells are observed within 24 h postinduction and, by 4 to 5 days postinduction, the majority of cells are found in massive clusters (see, for example, Fig. 6B). The data are shown for *rsp3* mutants, and the same phenotype is seen in *pf16* and *pf20* mutants (not shown). Arrows denote the posterior ends of cell bodies conjoined in clusters. (B) Motility mutants are blocked in the completion of cytokinesis. TbRSP3 cells incubated in the presence (+Tet, $n = 792$) or absence (−Tet, $n = 676$) of drug were examined by phase-contrast microscopy at 48 h. Cells were classified as described in the text. The percentage of cells in each category is indicated. In this experiment, two replicates were quantified (+Tet, $n = 393$ and $n = 399$; −Tet, $n = 334$ and $n = 342$), with the standard deviation indicated. These data are representative of three independent experiments.

to complete normal cell division and accumulated as clusters attached at their extreme posterior ends (Fig. 4A, and videos S6 to S7 in the supplemental material). Cleavage furrow formation in *T. brucei* initiates at the anterior end of the cell, between the tips of the new and old flagella, and then proceeds toward the posterior end, and in the final stages of cytokinesis daughter cells are only connected at their posterior ends (58). In wild-type cells, these daughter cells eventually pull apart before the next round of cytokinesis, while the motility mutants do not and therefore accumulate as larger and larger clusters. This defect was investigated more thoroughly in *rsp3* mutants, where reduced severity of flagellar paralysis allowed us to examine early aspects of the phenotype. Within 48 h postinduction, there was a decrease in the number of single cells and an increase in cell clusters containing two, three, four, and more than four conjoined cell bodies. Among the "double" cells (as defined in Materials and Methods and Fig. 4), there was no significant change in cells that had not initiated cytokinesis (Fig. 4B, double-1), whereas there was a significant increase in cells in the middle to late stages of cytokinesis (Fig. 4B, double-2). There was a modest decrease in the number of double-3 cells, perhaps indicating that cells undergoing cytokinesis must fully complete the double-2 stage before reaching the final stage. Analysis of cell cycle progression by immunofluorescence (see Materials and Methods) demonstrated that, aside from cells blocked in cytokinesis, there was no accumulation at any other stage of the cell cycle (not shown). These data, together with the fact that new rounds of cytokinesis can be initiated in "double" cells to produce "triple" and "quad" clusters, indicated that initiation of cytokinesis was not significantly affected but that daughter cells were unable to complete cell separation.

Knockdown of three different axonemal proteins resulted in loss of cell motility and a concomitant cytokinesis defect. Since the cytokinesis defect was unexpected, we sought to determine whether a similar defect would be observed when we targeted a nonaxonemal protein that is required for normal cell motility. PFR2 is one of two major proteins that comprise the kinetoplastid paraflagellar rod (5). Previously described PFR2 knockdown mutants had a reduced flagellar beat and were immotile at the cellular level (4, 7). These mutants exhibited a reduced growth rate compared to the wild type (6), although no specific cytokinesis defect was reported. To further investigate the connection between flagellar beat and cytokinesis, we generated two independent, tetracycline-inducible PFR2 knockdown mutants. Tetracycline induction led to a rapid and dramatic loss of PFR2 mRNA and protein in both mutants (Fig. 5A and B). The flagella of these mutants were able to beat, but beating was not sufficient to drive directional cell motility or significant cellular rotation (video S8 in the supplemental material).

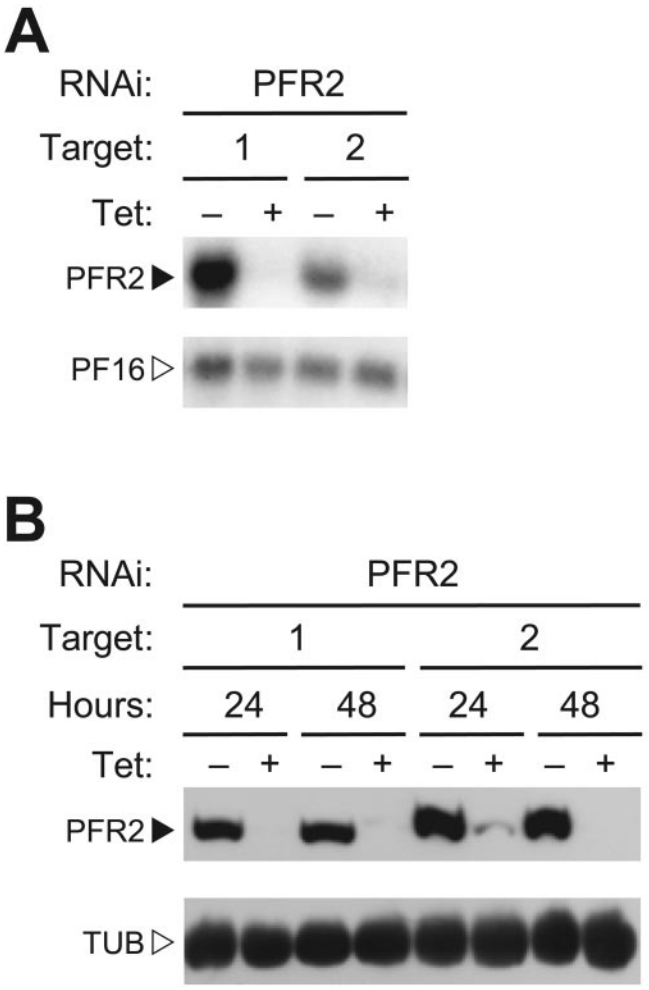

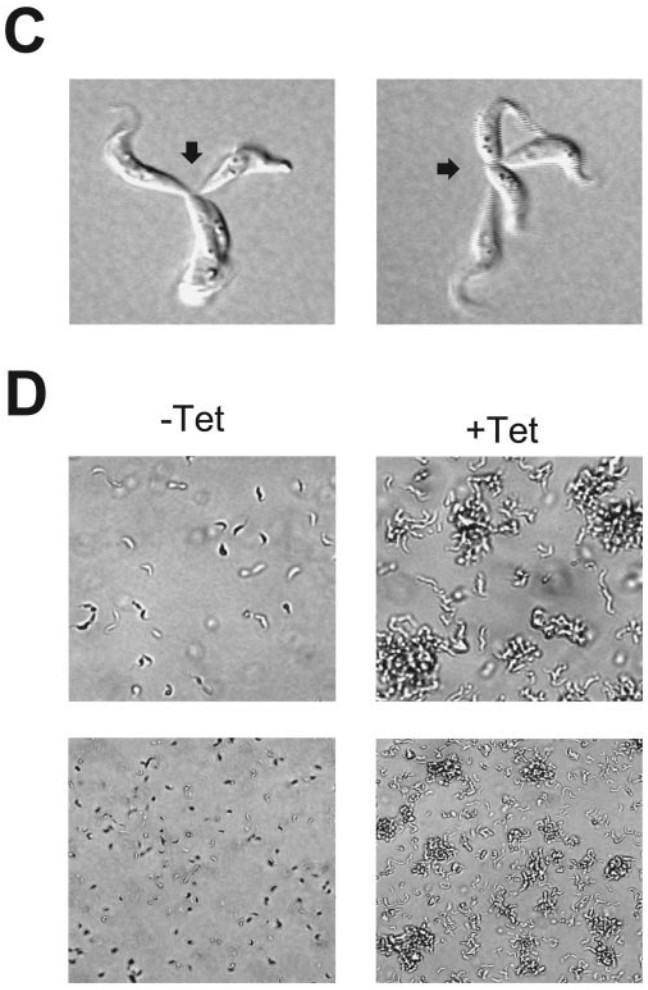

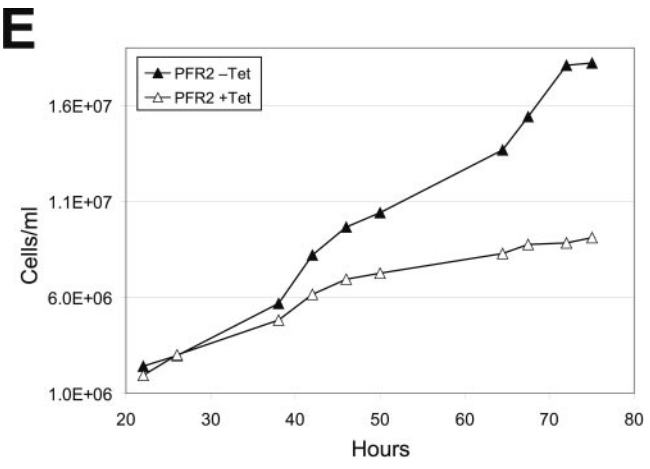

FIG. 5. *pfr2* mutants are defective in cytokinesis. (A) Northern blot demonstrating efficient RNAi knockdown of PFR2 in two independent knockdown cell lines. TbPFR2-1 (RNAi target 1) and TbPFR2-2 (RNAi target 2) cells were incubated in the presence (+) or absence (−) of tetracycline (Tet). Total RNA was prepared 24 h after the addition of tetracycline and subjected to Northern blot analysis with a PFR2 probe as indicated. The lower blot shows a loading control. (B) Western blot analysis of whole-cell lysates from TbPFR2-1 and TbPFR2-2 cells incubated in the presence (+) or absence (−) of tetracycline (Tet). Protein samples were prepared 24 and 48 h after the addition of tetracycline and subjected to Western blot analysis with an α-PFR2 monoclonal antibody (upper panel) or an α-β-tubulin monoclonal antibody as a loading control (lower panel). (C) DIC images of live *pfr2* mutants in multicellular clusters 48 h after the addition of tetracycline. TbPFR2-1 cells (left panel) and TbPFR2-2 cells (right panel) are shown. Arrows denote the posterior ends of cell bodies conjoined in clusters (each image is a frame taken from videos S9 and S10). (D) By 4 days postinduction, the majority of cells are found in massive multicellular clusters. Phase-contrast images of live cultures incubated with (+Tet) or without (−Tet) tetracycline are shown at ×20 magnification (upper panels) and ×10 magnification (lower panels). Images shown are from TbPFR2-1 cultures. Massive clusters are similarly observed in TbPFR2-2 cultures. (E) Growth curves of TbPFR2-1 cells grown in the presence (open symbols) or absence (filled symbols) of tetracycline, where tetracycline was added at time = 0.

Within 24 h of tetracycline induction, *pfr2* mutants began to accumulate as small clusters of cells attached at their posterior ends (Fig. 5C and videos S9 and S10 in the supplemental material), and a reduction in growth rate was observed (Fig. 5E). By 4 days postinduction, the majority of cells accumulated in massive clusters (Fig. 5D). Therefore, as was the case for central pair and radial spoke proteins, loss of PFR2 led to reduced flagellar beat, a loss of cell motility, and a concomitant block in cytokinesis.

Failure to complete cytokinesis in four independent motility mutants might reflect an active requirement for flagellar beat. Alternatively, the effect might be indirect, with an impaired

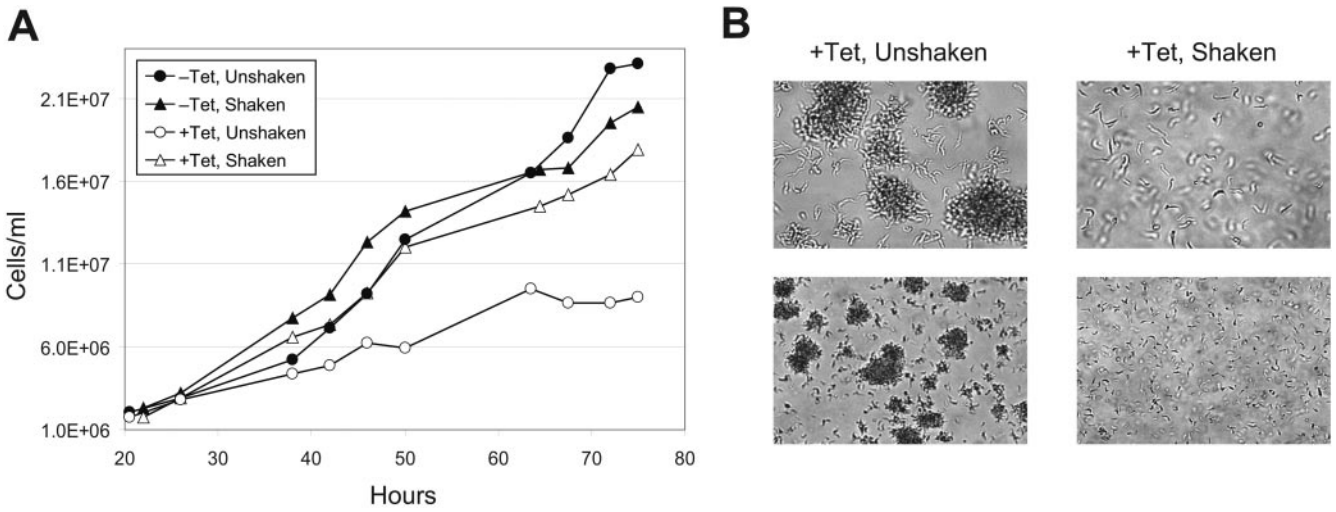

FIG. 6. Physical agitation of motility mutants rescues the cytokinesis defect. (A) Growth curves of TbRSP3 cells grown on a rotating shaker (triangles) or grown without shaking (circles), in the presence (open symbols) or absence (filled symbols) of tetracycline, where tetracycline was added at time = 0. (B) Phase-contrast images of live tetracycline-induced TbRSP3 cultures at 66 h postinduction. Cultures grown without shaking are shown in the left panels, while cultures grown with shaking are shown in the right panels. Images are shown at ×20 (upper panels) and ×10 (lower panels) magnification. Rotating also rescued the cytokinesis defect of *pf16* and *pf20* mutants (not shown).

beat causing internal structural defects that prevent the separation of daughter cells. If flagellar beat contributes directly to cell separation, gentle agitation of the mutant cultures may provide compensatory forces that allow cell division. On the other hand, if the effect is simply indirect, i.e., if flagellar paralysis simply distorts something inside the cell and as a result cells are inextricably intertwined, agitation is not expected to correct these defects and clusters should still form. Growth rate and cytokinesis were examined in motility mutants maintained normally ("unshaken") or on a rotating platform ("shaken"). Agitation of the culture completely rescued the cytokinesis defect, restored the growth rate (Fig. 6A), and prevented the formation of multicellular clusters (Fig. 6B).

Trypanin functions as part of a DRC in *T. brucei*. The motivation for generating radial spoke and central pair mutants was to determine whether a dynein regulatory system provides communication between CP/RS and axonemal dynein in *T. brucei*. The defining feature of DRC genes is that loss-of-function mutations in these genes suppress flagellar beat defects of central pair and radial spoke loss-of-function mutants (24). Tetracycline-inducible *pf16*/*tpn* and *rsp3*/*tpn* dual RNAi knockdown mutants were generated as described in Materials and Methods. Northern blot (Fig. 7A and B) and Western blot (Fig. 7C) analyses demonstrated that knockdown in double mutants was as efficient as knockdown in the corresponding single mutants.

The motility defect of *rsp3* and *pf16* single mutants in *T. brucei* is defined by three shared phenotypic characteristics: (i) sedimentation, (ii) an abnormal flagellar beat that is often restricted to the flagellar tip, and (iii) cytokinesis failure. In addition, flagellar beat in *pf16* mutants is restricted to an erratic twitching, resulting in a sharp curvature in the anterior cell body. The ability of trypanin knockdown to suppress any or all of these phenotypic characteristics was determined. Loss of trypanin did not suppress overall cellular movement defects, since the growth rate and sedimentation profiles of double mutants were similar to single mutants (not shown). However, the key feature of DRC suppression is improved flagellar beat, which was therefore examined with high-resolution phase contrast and DIC microscopy. Although the less-severe phenotype of *rsp3* mutants made it difficult to reliably detect improved flagellar beat, suppression of the *pf16* beat defect was immediately obvious in *pf16*/*tpn* double knockdown mutants (Fig. 8A and B, and videos S11 and S12 in the supplemental material). In contrast to the erratic flagellar twitch exhibited by *pf16* single mutants, *pf16*/*tpn* double mutants produced a sustained flagellar waveform and rarely twitched (compare videos S11 and S12 to video S3 in the supplemental material). Likewise, the curvature of the anterior cell body and flagellum, which is a hallmark of *pf16* single mutants, was reduced or absent in double mutants (Fig. 8A and B), most likely as a direct result of the more regular and controlled beating of the flagellum.

To demonstrate the suppression afforded by loss of trypanin, the phenotypic characteristics of these mutants were used to distinguish *pf16* single and *pf16*/*tpn* double mutants in a blind assay. Fifty separate samples of *pf16* and *pf16*/*tpn* mutants were visually inspected and mutants were accurately identified as single (*pf16*) or double (*pf16*/*tpn*) (Table 1). We also performed a quantitative analysis of flagellar motion to distinguish single and double mutants (Fig. 8C). A total of 100 *pf16* single mutants and 100 *pf16*/*tpn* double mutants were examined, and this analysis showed that flagella of most double mutants beat continuously, whereas single mutants do not (Fig. 8C). Therefore, loss of trypanin suppresses the erratic twitching and curved flagellum that are hallmarks of *pf16* mutants.

DISCUSSION

The *T. brucei* flagellum is important for many aspects of trypanosome cell biology and host-parasite interaction, yet our knowledge of the trypanosome flagellar apparatus is limited. In the present study, we advance understanding of this organelle

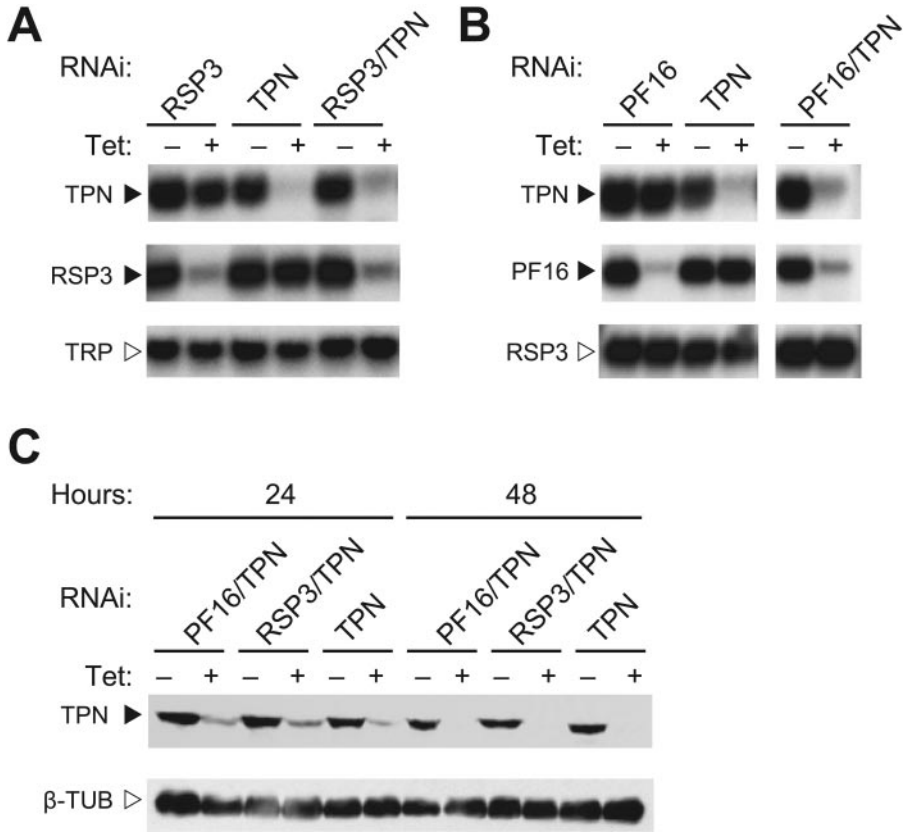

FIG. 7. *rsp3*/*tpn* and *pf16*/*tpn* double-knockdown mutants. (A and B) Northern blots demonstrating efficient RNAi knockdown of TPN, RSP3, and PF16 in single- and double-knockdown mutants. RNAi targets are indicated for each cell line, TbRSP3 (RSP3), TbTPN (TPN), TbPF16 (PF16), TbRSP3/TPN (RSP3/TPN), and TbPF16/TPN (PF16/TPN). Cells were incubated in the presence (+) or absence (−) of tetracycline (Tet) for 24 h, and total RNA was isolated and subjected to Northern blot analysis with TPN, RSP3, or PF16 probes, as indicated. The lower blots show loading controls. (C) Western blot analysis of whole-cell lysates from TbPF16/TPN (PF16/TPN), TbRSP3/TPN (RSP3/TPN), and TbTPN (TPN) cells incubated in the presence (+) or absence (−) of tetracycline (Tet). Protein samples were prepared 24 and 48 h after the addition of tetracycline and subjected to Western blot analysis with an α-TPN monoclonal antibody (upper panel) or an α-β-tubulin monoclonal antibody as a loading control (lower panel).

in four important ways. First, we establish a requirement for central pair and radial spoke components in *T. brucei* motility. Second, we demonstrate for the first time that the orientation of CP microtubules is fixed relative to outer doublet microtubules and that abnormal central pair orientation is correlated with severely defective motility. Third, our results demonstrate that flagellar motility contributes to normal cytokinesis in *T. brucei* and suggest that the flagellum has an active role in cell division, beyond its passive role as a structural and positional cue. Finally, we provide genetic evidence that the dynein regulatory complex, previously characterized only in algae, represents an evolutionarily conserved strategy for dynein regulation and that trypanin operates together with PF16 in a DRC-like regulatory system in *T. brucei*.

Trypanin is part of an evolutionarily conserved dynein regulatory system. Many cellular functions are dependent upon correct spatial and temporal regulation of dynein motors, and identification of the proteins and mechanisms underlying this regulation represents a major challenge in cell biology. In *C. reinhardtii*, the DRC functions as part of a mechanochemical signal transduction pathway that regulates the axonemal dynein in response to signals from central pair microtubules and radial spokes (24, 43, 44, 55). DRC components are defined through their genetic interaction with central pair components. Specifically, loss-of-function DRC mutations suppress flagellar beat defects of central pair loss-of-function mutants (24). Using dual RNAi knockdown, we show that the loss of trypanin suppresses the flagellar beat defects of a central pair (*pf16*) knockdown mutant in *T. brucei*, demonstrating a genetic interaction between trypanin and PF16. Therefore, trypanin meets the following criteria of a DRC component: (i) trypanin loss suppresses a central pair beat defect without restoring expression of the central pair protein, (ii) trypanin single knockdown mutants exhibit a motility defect indicative of abnormal dynein regulation (26), (iii) trypanin is stably associated with flagellar axonemes (19), and (iv) is distributed along the length of the flagellum (26). Taken together, these data show that trypanin functions as part of a DRC-like regulatory system in African trypanosomes. Although we did not readily detect a genetic interaction between RSP3 and trypanin, this is probably because the less severe *rsp3* phenotype makes suppression too subtle to detect.

Trypanin single-knockdown mutants are incapable of directional cell motility but have an actively beating flagellum and

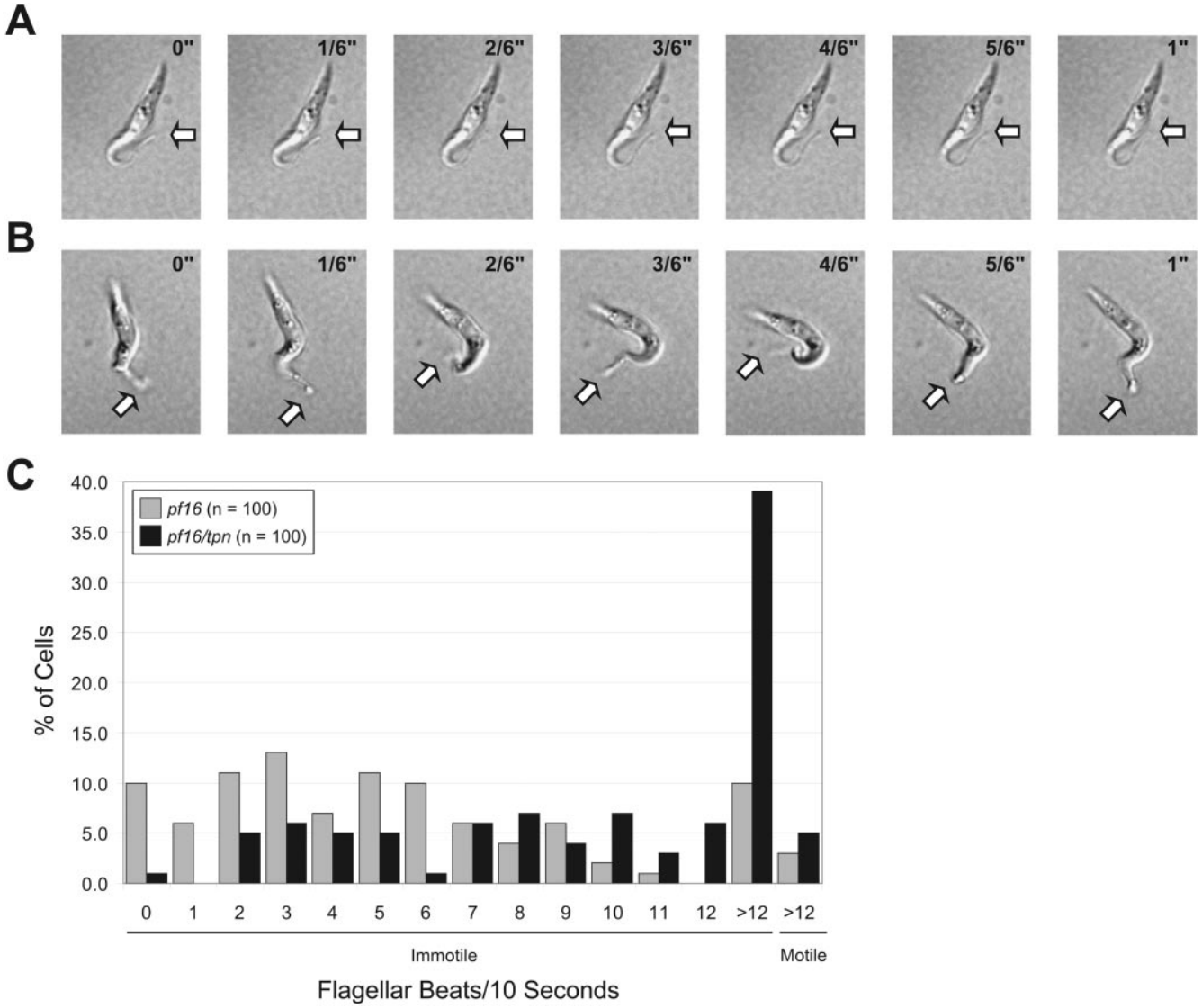

FIG. 8. Loss of trypanin suppresses the flagellar beat defect of a central pair mutant. Images show a time-lapse series of *pf16* single mutants (A) and *pf16*/*tpn* double mutants (B), taken every 1/6 of a second over a 1-s time period. All cells are shown with their anterior ends oriented downward, with arrows indicating the position of the flagellar tip. The hallmark of *pf16* single mutants is an S-shaped curvature of the anterior portion of the cell body and flagellar tip, accompanied by an abnormal flagellar beat (see text and video S3 in the supplemental material). *pf16*/*tpn* double mutants do not typically exhibit this anterior curvature and sustain a more normal flagellar beat (compare videos S11 and S12 with video S3 in the supplemental material). (C) Quantitative analysis of flagellar beating in *pf16* single mutant and *pf16*/*tpn* double mutant cultures. A total of 100 random cells from each cell line were analyzed 48 h after the addition of tetracycline. The number of beats at the flagellar tip, up to 12 or greater than 12 (>12), during a 10-s period were quantified for each cell. Overall, cellular movements in this time period were also analyzed, and cells that exhibited no net movement (Immotile) or net movement (Motile) are indicated. Note that while this quantitative assay clearly demonstrates suppression of *pf16* defects, it does not reflect the improved quality of beat in the double mutant. For example, although some *pf16* and *pf16*/*tpn* mutants fall into the same ">12" quantitative category, there are obvious qualitative differences in flagellar motion between these mutants (e.g., compare videos S11 and S12 with video S4 in the supplemental material).

are able to spin and tumble in place (26). Interestingly, a tumbling motion similar to the trypanin knockdown phenotype is also observed transiently in wild-type cells since they alternate between directional runs and random tumbles (18, 26). Therefore, the DRC of trypanosomes may provide a clutch-like regulatory mechanism that can be engaged for directional movement or disengaged for random tumbling. In bacteria, this type of behavior is exploited to drive changes in taxis in response to environmental cues (33).

A DRC function for trypanin is also supported by the localization of trypanin along the flagellum and may explain the flagellum attachment defect of trypanin knockdown mutants. The *T. brucei* flagellum is directly connected to the cell body along its length and trypanin knockdown mutants exhibit partial flagellar detachment (26). This defect is more pronounced upon the removal of cellular membranes, suggesting that the loss of trypanin compromises the structural integrity of flagellum attachment complexes (26). Since the DRC functions in

TABLE 1. Blind assay of single and double mutants[a]

Mutant	No. of cultures correctly identified/total no. tested (%)
Single (*pf16*)	20/22 (91)
Double (*pf16*/*tpn*)	27/28 (96)
Total	47/50 (94)

[a] Four independent cultures of *pf16* single mutants (TbPF16) and *pf16*/*tpn* double mutants (TbPF16/TPN) were induced with tetracycline for 48 h and divided among 50 different culture flasks. Each of these 50 flasks were visually examined blindly without knowledge of either the identity of the mutant (single or double) or how many flasks of each mutant were present. Samples were scored as single or double mutants based on the phenotypic characteristics defined in the text.

beat regulation, flagellum detachment in *tpn* knockdown mutants might be an indirect consequence of the motility defect, as previously suggested (55), rather than a direct consequence of the loss of trypanin. These two explanations are not mutually exclusive, and a third possibility is that trypanin functions in both capacities. The 96-nm periodicity of the DRC along the axoneme in *C. reinhardtii* (16) is the same as the periodicity of the flagellum attachment complexes in *T. brucei* (67). Therefore, the DRC or an associated structure might be exploited to serve a secondary function as an axonemal attachment site. Distinguishing between these possibilities will require more precise ultrastructural localization of trypanin and the DRC in *T. brucei*.

Further analysis of flagellar dynein regulation in *T. brucei* will be of tremendous interest, particularly since the trypanosome genome also contains a trypanin paralogue, TRP (for trypanin-related protein [see Materials and Methods]). TRP mRNA is not targeted by trypanin RNAi (Fig. 7A) and the contribution of TRP to dynein regulation remains to be determined. Interestingly, genes for both trypanin and TRP are found in other kinetoplastids, whereas *C. reinhardtii* and humans have only a single trypanin homologue (K. L. Hill, unpublished observation). The presence of a paraflagellar rod in kinetoplastids imparts structural asymmetry to the axoneme, since outer doublets four through seven are physically linked to the paraflagellar rod (5). This asymmetric arrangement undoubtedly imposes unique regulatory demands, and perhaps this need is met with two distinct dynein regulatory systems, one containing trypanin and the other containing TRP.

Radial spoke and central pair proteins are required for flagellar motility in *T. brucei*. We identified *T. brucei* RSP3, PF16, and PF20 homologues as single-copy genes in the *T. brucei* genome. Knockdown of each of these genes results in severely defective motility. Ultrastructural analysis demonstrates loss of radial spokes in *rsp3* mutants and abnormal central pair orientation in *pf16* and *pf20* mutants. In vitro studies with reactivated axonemes show that the position of the C1 microtubule of the central pair correlates with the position of active dyneins in *C. reinhardtii* (71, 72). Hence, the restricted orientation of central pair microtubules, together with the aberrant central pair orientation in *pf16* and *pf20* mutants, supports the idea that all dyneins around the circumference of the axoneme do not receive the same regulatory inputs in *T. brucei*. It is possible that the abnormal central pair orientation in *T. brucei pf16* and *pf20* mutants leads to aberrant dynein activity and abnormal motility, but currently we do not know whether abnormal central pair orientation is the cause or the consequence of the motility defect. We did not observe a loss of central pair microtubules in intact cells (Fig. 3) or demembranated flagella (not shown) from *pf16* or *pf20* mutants. In contrast, *pf16* and *pf20* deficiency in *C. reinhardtii* (1, 15) and mice (56, 77) manifests as instability of central pair microtubules, although the precise function of these proteins is not known. Interestingly, loss of central pair microtubules in *C. reinhardtii pf16* mutants is observed in demembranated axonemes but not in intact cells (15), indicating that something other than the absence of the central pair is responsible for the motility defect. By demonstrating that the presence of central pair microtubules is not sufficient for motility in *T. brucei*, our results also extend the findings of McKean et al. (35), who demonstrated that complete ablation of the central pair apparatus in *T. brucei* by gamma tubulin knockdown disrupts cell motility.

A rudimentary beat is often observed in the flagellar tips of *rsp3*, *pf16*, and *pf20* mutants. Since the flagellar beat in *T. brucei* initiates at the tip (69, 70), it thus appears that these mutants are able to initiate but not propagate flagellar beat. The pronounced curvature of *pf16* and *pf20* mutants likely also results from the inability to sustain flagellar beat, since it is reduced or absent in *pf16*/*tpn* double mutants and *rsp3* single mutants. The twitching and curved flagella seen in *T. brucei pf16* and *pf20* mutants is similar to the twitching and curved flagella of sperm from *pf16* knockout mice (56) and *pf20* chimeric mice (76). Twitching and phenotypic heterogeneity is also observed in *C. reinhardtii pf16* and *pf20* loss-of-function mutants (1, 15), suggesting that residual flagellar movement is independent of PF16 and PF20 and is not simply due to incomplete knockdown.

Radial spokes are composed of an estimated 23 proteins (75), with a surprisingly large number containing predicted regulatory domains, supporting the emerging concept that spokes play important roles in signal transduction and are not simply structural components of the flagellum (62). The central pair apparatus is also composed of at least 23 proteins (1, 15). By establishing a requirement for radial spoke and central pair proteins in trypanosome motility, our results facilitate structure-function analyses by aiding in rational selection of key amino acids to target with site-directed mutagenesis. The repertoire of tools available for molecular genetic manipulation in *T. brucei*, including targeted gene knockouts and inducible RNAi knockdowns, makes these parasites a powerful system for elucidating the function of these and other (3, 31) candidate motility genes.

Flagellar motility is required for cytokinesis. An unanticipated finding from our studies is that flagellar motility is required for normal cell division. *rsp3*, *pf16*, *pf20*, and *pfr2* knockdown mutants are each blocked at the final stage of cell separation but can reinitiate cytokinesis multiple times. The loss of RSP3, PF16, PF20, or PFR2 affects distinct substructures within the flagellum, and in all four mutants defective flagellar motility precedes the block in cytokinesis. Therefore, flagellar motility itself, rather than a specific flagellar substructure, is required for cytokinesis.

Other motility mutants have been described in *T. brucei*. Since those that are nonviable are also defective in critical structures such as the mitotic spindle (35) or flagellum attach-

TABLE 2. Cell motility and cytokinesis phenotypes

Phenotype[b]	Strain(s)[a]			
				
	Wild type	*tpn*	*pf16* and *pf20*	*pf16*/*tpn*, *rsp3*, and *pfr2*
Flagellar beat	+	+	−	+
Forward motility	+	−	−	−
Cellular rotation	+	+	−	−
Cytokinesis	+	+	−	−

[a] Schematic illustration of RNAi knockdown strains used in this study (*pf16*, *pf20*, *pf16*/*tpn*, *rsp3*, and *pfr2*), as well as the *tpn* knockdown (26) and wild-type strains. Flagella are shown in blue. A circular red arrow denotes cellular rotation, and a straight red arrow denotes directional motility.

[b] The phenotypes of each strain, as described in the text, are listed. All mutants that are incapable of cellular rotation are also defective in cytokinesis.

ment zone (28, 30), it is difficult to assess the relative contribution of flagellar beat to the lethal phenotype. PFR2 knockdown mutants, *snl-1* (7) and *snl-2* (4), have been described previously that exhibit severely reduced flagellar beat. These mutants are viable but grow more slowly than the wild type (6). Cytokinesis was not specifically examined in the previous studies, although one report indicates that *snl-2* cells divide normally (4). Reexamination of these mutants demonstrates they form multicellular clusters, albeit not to the extent seen in the *pfr2* mutants obtained in the current study (P. Bastin, personal communication). The reason for the difference in severity is not entirely clear, but both *snl-1* (7) and *snl-2* (4) were isolated under conditions in which PFR2 dsRNA is expressed. Hence, there is selective pressure for compensation to allow outgrowth of these mutants, and the difference in severity may be due to differences in the extent of flagellar beating and/or other compensating factors. Consistent with this explanation, transfection of the *snl-2* plasmid into a cell line that lacks a tetracycline repressor and therefore expresses high levels of the PFR2 dsRNA gave poor transfection efficiency, and the few transfectants obtained had severe cytokinesis defects (P. Bastin, personal communication). An independent *pfr2* mutant generated utilizing an intermolecular dsRNA is viable (14) but also forms multicellular clusters (P. Bastin, personal communication). Finally, attempts to generate a PFR2 knockout via gene disruption in *T. brucei* have failed (25), a finding consistent with the idea that the PFR2 gene is essential. Therefore, the combined data support a requirement for flagellar motility in cytokinesis in *T. brucei*.

The cytokinesis defect of motility mutants might reflect a direct or indirect role for flagellar beat or a combination of direct and indirect roles. Several lines of evidence suggest that a direct role is at least partially responsible. The initial defect is marked by an accumulation of cells connected at their extreme posterior ends. Hence, cleavage furrow ingression and progression along the flagellum attachment zone is normal, and cell separation fails at the posterior end. Indeed, daughter cells are sometimes connected by only a thin string of membrane (data not shown). It is difficult to envision internal structural defects preventing cell separation at this stage of division. This is very different than the phenotype observed in *fla1* mutants, where disruption of flagellum attachment structures prevents the initiation of cytokinesis (30). Flagellar motility can influence positioning of the kinetoplast (unpublished observation), which is connected to the flagellar basal body (39), and it is possible that indirect effects also contribute to the cytokinesis defect, particularly several days postinduction. However, the finding that physical forces provided by mechanical rotation of cultures completely rescues the cytokinesis defect demonstrates that no physical barrier precludes cell separation and supports the idea that physical forces provided by the flagellar beat contribute to cell division. Mechanical forces also contribute to cytokinesis in animal cells (50). In wild-type trypanosomes at the final stage of cytokinesis, daughter cells are opposing one another, with their flagella pointing in opposite directions (video S13 in the supplemental material) (58). Since there is no compelling evidence for an actin/myosin II contractile ring at the cleavage furrow in *T. brucei* (15), exploiting directional and rotational pulling forces imparted by flagellar beating would be a convenient way to aid in the final separation of dividing cells. A similar phenomenon, termed rotokinesis, whereby ciliary driven cell motility and perhaps cell rotation assists in the separation of daughter cells has been described in *Tetrahymena thermophila* (8). Note that a universal feature of trypanosome motility mutants that fail in cytokinesis is that they do not rotate. In contrast, flagellar beat drives vigorous cellular rotation in wild-type cells and in trypanin single mutants, which divide normally (Table 2 and compare videos S13 and S14 in the supplemental material) (26).

Summary. Defects in ciliary motility are linked to wide variety of inherited human diseases (2, 27, 63) and a better understanding of flagellar motility is critical for the development of new strategies to treat these diseases. Although the structural features of the flagellum have been studied extensively and are considered to be well conserved, regulatory mechanisms that control flagellar beat are not well understood in any organism. In the present study, we demonstrate that the DRC is an evolutionarily conserved dynein regulatory system and that altered orientation of central pair microtubules is linked to cell motility defects in vivo. We also provide the first evidence that flagellar motility is required for cell division in *T. brucei*, the causative agent of African sleeping sickness. This suggests that the numerous enzymatic activities that drive the beating of the eukaryotic flagellum, such as ATPases, phosphatases, and kinases (48), represent candidate drug targets for treatment of this fatal disease.

ACKNOWLEDGMENTS

This study was supported by grants from the National Institutes of Health (R01AI52348) and Ellison Medical Foundation (ID-NS-0148-03) to K.L.H. K.S.R. is a recipient of a USPHS National Research Service Award (GM07104). A.G.L. was supported by a MARC U*STAR traineeship from the NIH/NIGMS (GM08563).

We are extremely grateful to Bryce McLelland for preparation of trypanin monoclonal antibodies and all of his excellent technical assistance and invigorating discussions. We thank Philip Postovoit and Joel Schonbrun for assistance with video imaging. We thank Philippe Bastin for stimulating discussions and sharing unpublished work, Keith Gull for antibodies against PFRA, George Cross for the 29-13 cell line, and John Donelson for the p2T7-Ti plasmid. We thank Nancy Sturm for many helpful and stimulating discussions on the manuscript and are grateful to coworkers and members of our laboratory for critical reading of the manuscript and thoughtful comments on this work.

REFERENCES

1. **Adams, G. M., B. Huang, G. Piperno, and D. J. Luck.** 1981. Central-pair microtubular complex of *Chlamydomonas flagella*: polypeptide composition as revealed by analysis of mutants. J. Cell Biol. **91:**69–76.
2. **Afzelius, B. A.** 2004. Cilia-related diseases. J. Pathol. **204:**470–477.
3. **Avidor-Reiss, T., A. M. Maer, E. Koundakjian, A. Polyanovsky, T. Keil, et al.** 2004. Decoding cilia function: defining specialized genes required for compartmentalized cilia biogenesis. Cell **117:**527–539.
4. **Bastin, P., K. Ellis, L. Kohl, and K. Gull.** 2000. Flagellum ontogeny in trypanosomes studied via an inherited and regulated RNA interference system. J. Cell Sci. **113:**3321–3328.
5. **Bastin, P., K. R. Matthews, and K. Gull.** 1996. The paraflagellar rod of Kinetoplastida: solved and unsolved questions. Parasitol. Today **12:**302–307.
6. **Bastin, P., T. J. Pullen, T. Sherwin, and K. Gull.** 1999. Protein transport and flagellum assembly dynamics revealed by analysis of the paralysed trypanosome mutant *snl-1*. J. Cell Sci. **112:**3769–3777.
7. **Bastin, P., T. Sherwin, and K. Gull.** 1998. Paraflagellar rod is vital for trypanosome motility. Nature **391:**548.
8. **Brown, J. M., C. Hardin, and J. Gaertig.** 1999. Rotokinesis, a novel phenomenon of cell locomotion-assisted cytokinesis in the ciliate *Tetrahymena thermophila*. Cell Biol. Int. **23:**841–848.
9. **Cachon, J., M. Cachon, M.-P. Cosson, and J. Cosson.** 1988. The paraflagellar rod: a structure in search of a function. Biol. Cell **63:**169–181.

9a. **Colantonio, J. R., J. M. Bekker, et al.** 2006. Expanding the role of the dynein regulatory complex to non-axonemal functions; association of Gas11 with the Golgi apparatus. Traffic [Online.] doi:10.1111/j.1600-0854.2006.00411.x.

10. **Chu, D. T., and M. W. Klymkowsky.** 1989. The appearance of acetylated alpha-tubulin during early development and cellular differentiation in *Xenopus*. Dev. Biol. **136:**104–117.
11. **Cosson, J.** 1996. A moving image of flagella: news and views on the mechanisms involved in axonemal beating. Cell. Biol. Int. **20:**83–94.
12. **Curry, A. M., and J. L. Rosenbaum.** 1993. Flagellar radial spoke: a model molecular genetic system for studying organelle assembly. Cell Motil. Cytoskel. **24:**224–232.
13. **Diener, D. R., L. H. Ang, and J. L. Rosenbaum.** 1993. Assembly of flagellar radial spoke proteins in *Chlamydomonas*: identification of the axoneme binding domain of radial spoke protein 3. J. Cell Biol. **123:**183–190.
14. **Durand-Dubief, M., L. Kohl, and P. Bastin.** 2003. Efficiency and specificity of RNA interference generated by intra- and intermolecular double stranded RNA in *Trypanosoma brucei*. Mol. Biochem. Parasitol. **129:**11–21.
15. **Dutcher, S. K., B. Huang, and D. J. Luck.** 1984. Genetic dissection of the central pair microtubules of the flagella of *Chlamydomonas reinhardtii*. J. Cell Biol. **98:**229–236.
16. **Gardner, L. C., E. O'Toole, C. A. Perrone, T. Giddings, and M. E. Porter.** 1994. Components of a "dynein regulatory complex" are located at the junction between the radial spokes and the dynein arms in *Chlamydomonas* flagella. J. Cell Biol. **127:**1311–1325.
17. **Gull, K.** 1999. The cytoskeleton of trypanosomatid parasites. Annu. Rev. Microbiol. **53:**629–655.
18. **Hill, K. L.** 2003. Mechanism and biology of trypanosome cell motility. Eukaryot. Cell **2:**200–208.
19. **Hill, K. L., N. R. Hutchings, P. M. Grandgenett, and J. E. Donelson.** 2000. T Lymphocyte triggering factor of African trypanosomes is associated with the flagellar fraction of the cytoskeleton and represents a new family of proteins that are present in several divergent eukaryotes. J. Biol. Chem. **275:**39369–39378.
20. **Hill, K. L., N. R. Hutchings, D. G. Russell, and J. E. Donelson.** 1999. A novel protein targeting domain directs proteins to the anterior cytoplasmic face of the flagellar pocket in African trypanosomes. J. Cell Sci. **112:**3091–3101.
21. **Hill, K. L., H. H. Li, J. Singer, and S. Merchant.** 1991. Isolation and structural characterization of the *Chlamydomonas reinhardtii* gene for cytochrome c6: analysis of the kinetics and metal specificity of its copper-responsive expression. J. Biol. Chem. **266:**15060–15067.
22. **Holwill, M. E.** 1974. Some physical aspects of the motility of ciliated and flagellated microorganisms. Sci. Prog. **61:**63–80.
23. **Holwill, M. E. J.** 1965. The motion of *Strigomona oncopelti*. J. Exp. Biol. **42:**125–137.
24. **Huang, B., Z. Ramanis, and D. J. Luck.** 1982. Suppressor mutations in *Chlamydomonas* reveal a regulatory mechanism for flagellar function. Cell **28:**115–124.
25. **Hungerglaser, I., and T. Seebeck.** 1997. Deletion of the genes for the paraflagellar rod protein PFR-A in *Trypanosoma brucei* is probably lethal. Mol. Biochem. Parasitol. **90:**347–351.
26. **Hutchings, N. R., J. E. Donelson, and K. L. Hill.** 2002. Trypanin is a cytoskeletal linker protein and is required for cell motility in African trypanosomes. J. Cell Biol. **156:**867–877.
27. **Ibanez-Tallon, I., N. Heintz, and H. Omran.** 2003. To beat or not to beat: roles of cilia in development and disease. Hum. Mol. Genet. **12**(Spec. No. 1)**:**R27–R35.
28. **Kohl, L., D. Robinson, and P. Bastin.** 2003. Novel roles for the flagellum in cell morphogenesis and cytokinesis of trypanosomes. EMBO J. **22:**5336–5346.
29. **Kohl, L., T. Sherwin, and K. Gull.** 1999. Assembly of the paraflagellar rod and the flagellum attachment zone complex during the *Trypanosoma brucei* cell cycle. J. Eukaryot. Microbiol. **46:**105–109.
30. **LaCount, D. J., B. Barrett, and J. E. Donelson.** 2002. *Trypanosoma brucei* FLA1 is required for flagellum attachment and cytokinesis. J. Biol. Chem. **277:**17580–17588.
31. **Li, J. B., J. M. Gerdes, C. J. Haycraft, Y. Fan, T. M. Teslovich, et al.** 2004. Comparative genomics identifies a flagellar and basal body proteome that includes the BBS5 human disease gene. Cell **117:**541–552.
32. **Lindemann, C. B., and K. S. Kanous.** 1997. A model for flagellar motility. Int. Rev. Cytol. **173:**1–72.
33. **Manson, M. D., J. P. Armitage, J. A. Hoch, and R. M. Macnab.** 1998. Bacterial locomotion and signal transduction. J. Bacteriol. **180:**1009–1022.
34. **Mastronarde, D. N., E. T. O'Toole, K. L. McDonald, J. R. McIntosh, and M. E. Porter.** 1992. Arrangement of inner dynein arms in wild-type and mutant flagella of *Chlamydomonas*. J. Cell Biol. **118:**1145–1162.
35. **McKean, P. G., A. Baines, S. Vaughan, and K. Gull.** 2003. Gamma-tubulin functions in the nucleation of a discrete subset of microtubules in the eukaryotic flagellum. Curr. Biol. **13:**598–602.
36. **Mitchell, D. R.** 2000. *Chlamydomonas* flagella. J. Phycol. **36:**261–273.
37. **Moreira-Leite, F. F., T. Sherwin, L. Kohl, and K. Gull.** 2001. A trypanosome structure involved in transmitting cytoplasmic information during cell division. Science **294:**610–612.
38. **Ngo, H., C. Tschudi, K. Gull, and E. Ullu.** 1998. Double-stranded RNA induces mRNA degradation in *Trypanosoma brucei*. Proc. Natl. Acad. Sci. USA **95:**14687–14692.
39. **Ogbadoyi, E. O., D. R. Robinson, and K. Gull.** 2003. A high-order transmembrane structural linkage is responsible for mitochondrial genome positioning and segregation by flagellar basal bodies in trypanosomes. Mol. Biol. Cell **14:**1769–1779.
40. **Omoto, C. K., I. R. Gibbons, R. Kamiya, C. Shingyoji, K. Takahashi, et al.** 1999. Rotation of the central pair microtubules in eukaryotic flagella. Mol. Biol. Cell **10:**1–4.
41. **Omoto, C. K., T. Yagi, E. Kurimoto, and R. Kamiya.** 1996. Ability of paralyzed flagella mutants of *Chlamydomonas* to move. Cell Motil. Cytoskel. **33:**88–94.
42. **Pepin, J., and J. E. Donelson.** 1999. African trypanosomiasis (sleeping sickness), p. 774–784. I*n* R. Guerrant, D. H. Walker, and P. F. Weller (ed.), Tropical infectious diseases: principles, pathogens and practice, vol. 1. Churchill Livingstone, Philadelphia, Pa.
43. **Piperno, G., K. Mead, M. LeDizet, and A. Moscatelli.** 1994. Mutations in the "dynein regulatory complex" alter the ATP-insensitive binding sites for inner arm dyneins in *Chlamydomonas axonemes*. J. Cell Biol. **125:**1109–1117.
44. **Piperno, G., K. Mead, and W. Shestak.** 1992. The inner dynein arms I2 interact with a "dynein regulatory complex" in *Chlamydomonas* flagella. J. Cell Biol. **118:**1455–1463.
45. **Poltera, A. A.** 1985. Pathology of human African trypanosomiasis with reference to experimental African trypanosomiasis and infections of the central nervous system. Br. Med. Bull. **41:**169–174.
46. **Porter, M. E., J. A. Knott, L. C. Gardner, D. R. Mitchell, and S. K. Dutcher.** 1994. Mutations in the SUP-PF-1 locus of *Chlamydomonas reinhardtii* identify a regulatory domain in the beta-dynein heavy chain. J. Cell Biol. **126:**1495–1507.
47. **Porter, M. E., J. Power, and S. K. Dutcher.** 1992. Extragenic suppressors of paralyzed flagellar mutations in *Chlamydomonas reinhardtii* identify loci that alter the inner dynein arms. J. Cell Biol. **118:**1163–1176.
48. **Porter, M. E., and W. S. Sale.** 2000. The 9+2 axoneme anchors multiple inner arm dyneins and a network of kinases and phosphatases that control motility. J. Cell Biol. **151:**F37–F42.
49. **Redmond, S., J. Vadivelu, and M. C. Field.** 2003. RNAit: an automated

web-based tool for the selection of RNAi targets in *Trypanosoma brucei*. Mol. Biochem. Parasitol. **128:**115–118.
50. **Reichl, E. M., J. C. Effler, and D. N. Robinson.** 2005. The stress and strain of cytokinesis. Trends Cell Biol. **15:**200–206.
51. **Robinson, D., P. Beattie, T. Sherwin, and K. Gull.** 1991. Microtubules, tubulin, and microtubule-associated proteins of trypanosomes. Methods Enzymol. **196:**285–299.
52. **Robinson, D. R., and K. Gull.** 1991. Basal body movements as a mechanism for mitochondrial genome segregation in the trypanosome cell cycle. Nature **352:**731–733.
53. **Robinson, D. R., T. Sherwin, A. Ploubidou, E. H. Byard, and K. Gull.** 1995. Microtubule polarity and dynamics in the control of organelle positioning, segregation, and cytokinesis in the trypanosome cell cycle. J. Cell Biol. **128:**1163–1172.
54. **Rupp, G., E. O'Toole, L. C. Gardner, B. F. Mitchell, and M. E. Porter.** 1996. The *sup-pf-2* mutations of *Chlamydomonas* alter the activity of the outer dynein arms by modification of the gamma-dynein heavy chain. J. Cell Biol. **135:**1853–1865.
55. **Rupp, G., and M. E. Porter.** 2003. A subunit of the dynein regulatory complex in *Chlamydomonas* is a homologue of a growth arrest-specific gene product. J. Cell Biol. **162:**47–57.
56. **Sapiro, R., I. Kostetskii, P. Olds-Clarke, G. L. Gerton, G. L. Radice, et al.** 2002. Male infertility, impaired sperm motility, and hydrocephalus in mice deficient in sperm-associated antigen 6. Mol. Cell. Biol. **22:**6298–6305.
57. **Satir, P.** 1995. Landmarks in cilia research from Leeuwenhoek to us. Cell Motil. Cytoskel. **32:**90–94.
58. **Sherwin, T., and K. Gull.** 1989. The cell division cycle of *Trypanosoma brucei brucei*: timing of event markers and cytoskeletal modulations. Philos. Trans. R. Soc. Lond. Ser. B Biol. Sci. **323:**573–588.
59. **Smith, E. F., and P. A. Lefebvre.** 1996. PF16 encodes a protein with armadillo repeats and localizes to a single microtubule of the central apparatus in *Chlamydomonas* flagella. J. Cell Biol. **132:**359–370.
60. **Smith, E. F., and P. A. Lefebvre.** 1997. PF20 gene product contains WD repeats and localizes to the intermicrotubule bridges in *Chlamydomonas* flagella. Mol. Biol. Cell **8:**455–467.
61. **Smith, E. F., and W. S. Sale.** 1992. Regulation of dynein-driven microtubule sliding by the radial spokes in flagella. Science **257:**1557–1559.
62. **Smith, E. F., and P. Yang.** 2004. The radial spokes and central apparatus: mechano-chemical transducers that regulate flagellar motility. Cell Motil. Cytoskel. **57:**8–17.
63. **Snell, W. J., J. Pan, and Q. Wang.** 2004. Cilia and flagella revealed: from flagellar assembly in *Chlamydomonas* to human obesity disorders. Cell **117:** 693–697.
64. **Sugrue, P., M. R. Hirons, J. U. Adam, and M. E. Holwill.** 1988. Flagellar wave reversal in the kinetoplastid flagellate *Crithidia oncopelti*. Biol. Cell **63:**127–131.
65. **Thompson, J. D., D. G. Higgins, and T. J. Gibson.** 1994. CLUSTAL W: improving the sensitivity of progressive multiple sequence alignment through sequence weighting, position-specific gap penalties and weight matrix choice. Nucleic Acids Res. **22:**4673–4680.
66. **Van Den Abbeele, J., Y. Claes, D. van Bockstaele, D. Le Ray, and M. Coosemans.** 1999. *Trypanosoma brucei* spp. development in the tsetse fly: characterization of the post-mesocyclic stages in the foregut and proboscis. Parasitology **118:**469–478.
67. **Vickerman, K.** 1969. On the surface coat and flagellar adhesion in trypanosomes. J. Cell Sci. **5:**163–193.
68. **Vickerman, K., L. Tetley, K. A. Hendry, and C. M. Turner.** 1988. Biology of African trypanosomes in the tsetse fly. Biol. Cell **64:**109–119.
69. **Walker, P. J.** 1961. Organization of function in trypanosome flagella. Nature **189:**1017–1018.
70. **Walker, P. J., and J. C. Walker.** 1963. Movement of trypanosome flagella. J. Protozool. **10:**32.
71. **Wargo, M. J., M. A. McPeek, and E. F. Smith.** 2004. Analysis of microtubule sliding patterns in *Chlamydomonas* flagellar axonemes reveals dynein activity on specific doublet microtubules. J. Cell Sci. **117:**2533–2544.
72. **Wargo, M. J., and E. F. Smith.** 2003. Asymmetry of the central apparatus defines the location of active microtubule sliding in *Chlamydomonas* flagella. Proc. Natl. Acad. Sci. USA **100:**137–142.
73. **Williams, B. D., M. A. Velleca, A. M. Curry, and J. L. Rosenbaum.** 1989. Molecular cloning and sequence analysis of the *Chlamydomonas* gene coding for radial spoke protein 3: flagellar mutation pf-14 is an ochre allele. J. Cell Biol. **109:**235–245.
74. **Wirtz, E., S. Leal, C. Ochatt, and G. A. Cross.** 1999. A tightly regulated inducible expression system for conditional gene knockouts and dominant-negative genetics in *Trypanosoma brucei*. Mol. Biochem. Parasitol. **99:**89–101.
75. **Yang, P., D. R. Diener, J. L. Rosenbaum, and W. S. Sale.** 2001. Localization of calmodulin and dynein light chain LC8 in flagellar radial spokes. J. Cell Biol. **153:**1315–1326.
76. **Zhang, Z., I. Kostetskii, S. B. Moss, B. H. Jones, C. Ho, et al.** 2004. Haploinsufficiency for the murine orthologue of *Chlamydomonas* PF20 disrupts spermatogenesis. Proc. Natl. Acad. Sci. USA **101:**12946–12951.
77. **Zhang, Z., R. Sapiro, D. Kapfhamer, M. Bucan, J. Bray, et al.** 2002. A sperm-associated WD repeat protein orthologous to *Chlamydomonas* PF20 associates with Spag6, the mammalian orthologue of *Chlamydomonas* PF16. Mol. Cell. Biol. **22:**7993–8004.